Materials for fusion research

various type of coatings has to be developed for fusion reactors

ceramic coatings:

-The development of electrical insulating ceramic coatings has been conducted for reduction of MHD (magnetohydrodynamic) pressure drop of liquid Li breeder/coolant in the Li/Vanadiumalloy blanket system.

-The recent studies have confirmed that candidate materials of, Er_2O_3, Y_2O_3, AlN, $CaZrO_3$, Al_2O_3, etc., could maintain the chemical compatibility with highly corrosive high-temperature liquid Li during long-time exposure.
- These ceramic coatings should be resistant against induced conductivity by radiation.

Examples of induced conductivity by radiation for these insulators.

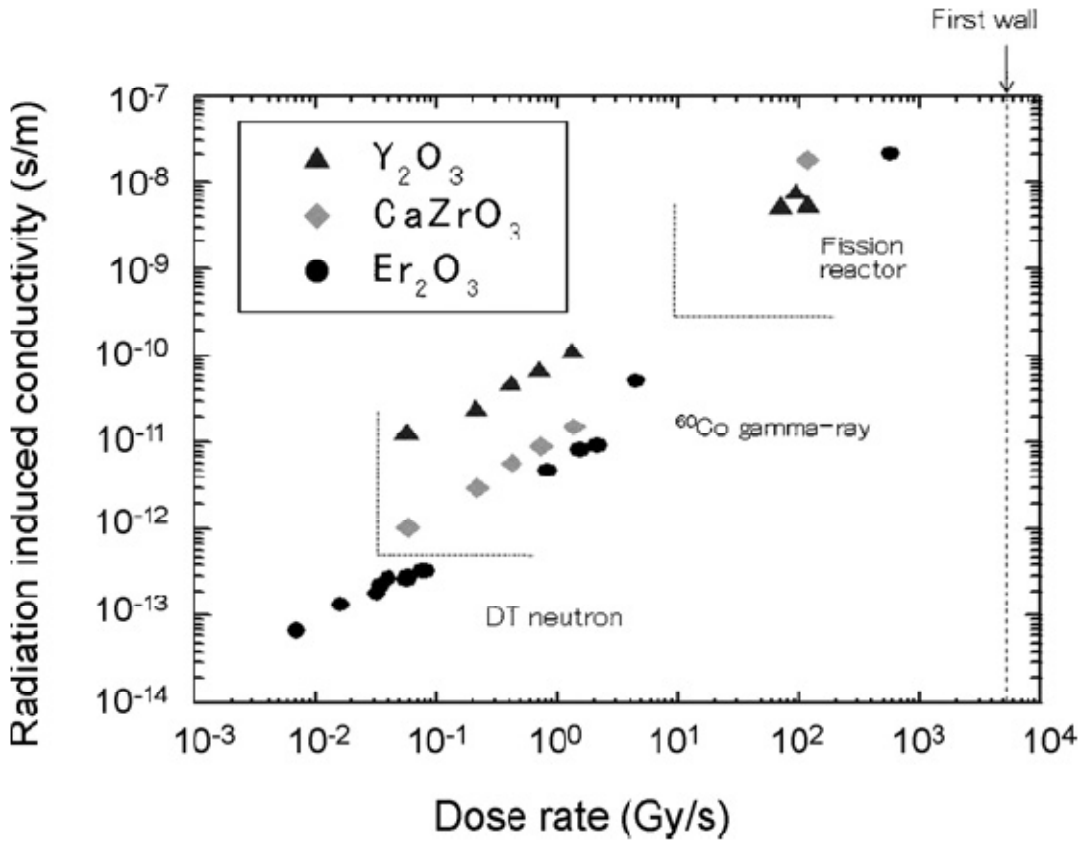

Fig. 5. Radiation-induced conductivities of bulk MHD coating materials. The irradiation and test temperature are between RT and 50 °C, except for fission reactor irradiation. Data presented here overlap in general with those in Fig. 1.

Walls coatings:

beryllium coatings (first wall in the thermonuclear power plants)

W-coated carbon/carbon composite (for diverter armor tiles of ITER)

These coatings should be:

a) adherent to the substrate and very compact

b) very resistant against high energy plasma interaction (ions, electrons, neutrons)

c) They should exhibit low erosion rate

Many technological approaches are to be optimized and implemented for preparation of these materials coating materials.

Perspective PVD and IPVD methods for these purposes are for example:

-magnetron sputtering deposition

-RF magnetron, pulsed HIPIMS magnetrons

-hollow cathode systems

-EB ARC deposition systems

-cathodic arc depositions

other IPVD methods

Sputtering systems fundamentals

The classical parallel plate DC glow discharge configuration operated in the normal mode called normal glow discharge (NGD)

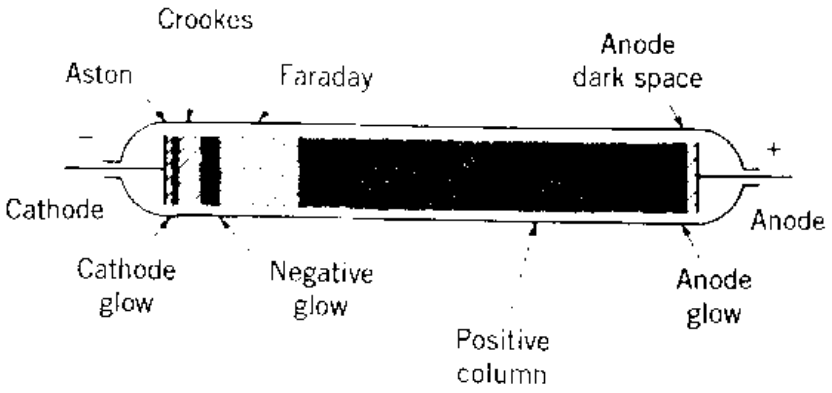

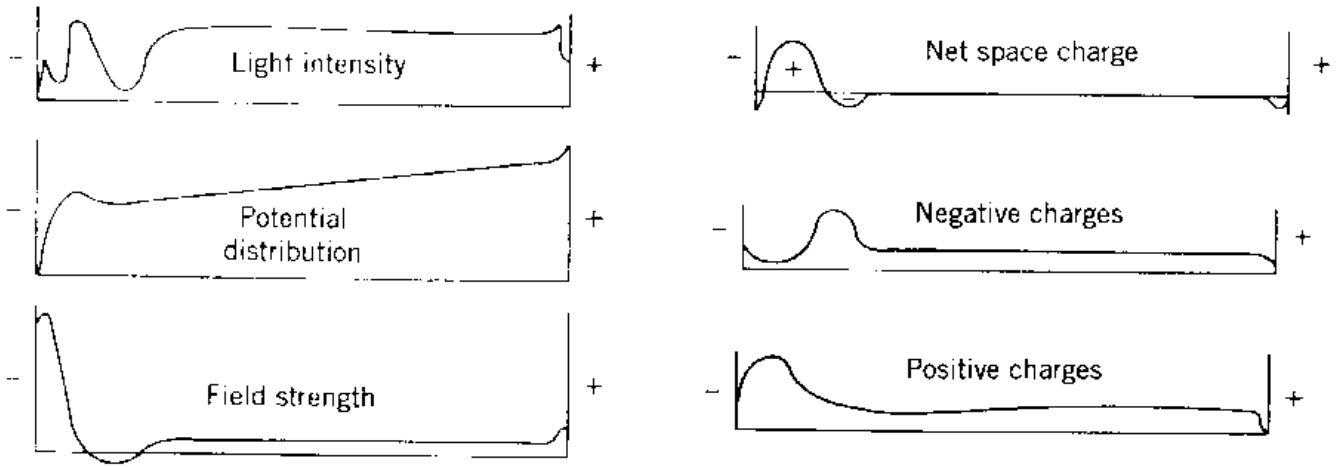

Lieberman, M. A. (Michael A.)
Principles of plasma discharges and materials processing / Michael A. Lieberman, Allan J. Lichtenberg.

the classical parallel plate DC glow discharge configuration operated in the normal mode called normal glow discharge (NGD)

The normal current density j_0:

$$j_0 = \frac{4\varepsilon_0 \mu_+ V_{cn}^2 (1+\gamma_i)}{d_n^3}$$

where V_{cn} is normal cathode voltage drop, μ_+ is ion mobility, γ_i ion –electron secondary emission coefficient a d_n is the length of cathode voltage drop.

When the total current increases the current density j_0 remains constant but the cathode spot will extend its area. This can continue only to the moment when the whole of cathode surface is covered by the active cathode spot. From this point for further discharge current increase, the NGD will transfer to anomalous glow discharge (AGD) accompanied by the increase of current density and the cathode voltage.

AGD is sometimes used in applications of thin films depositions by the cathode sputtering

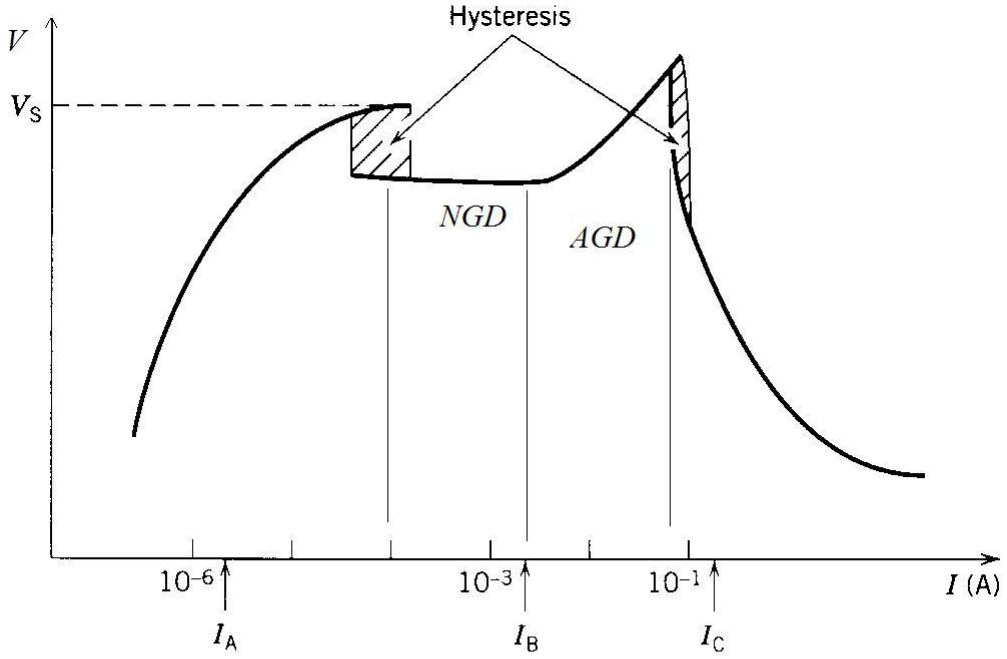

Typical voltage–current characteristic of a dc glow discharge.

DC cathode sputtering in AGD

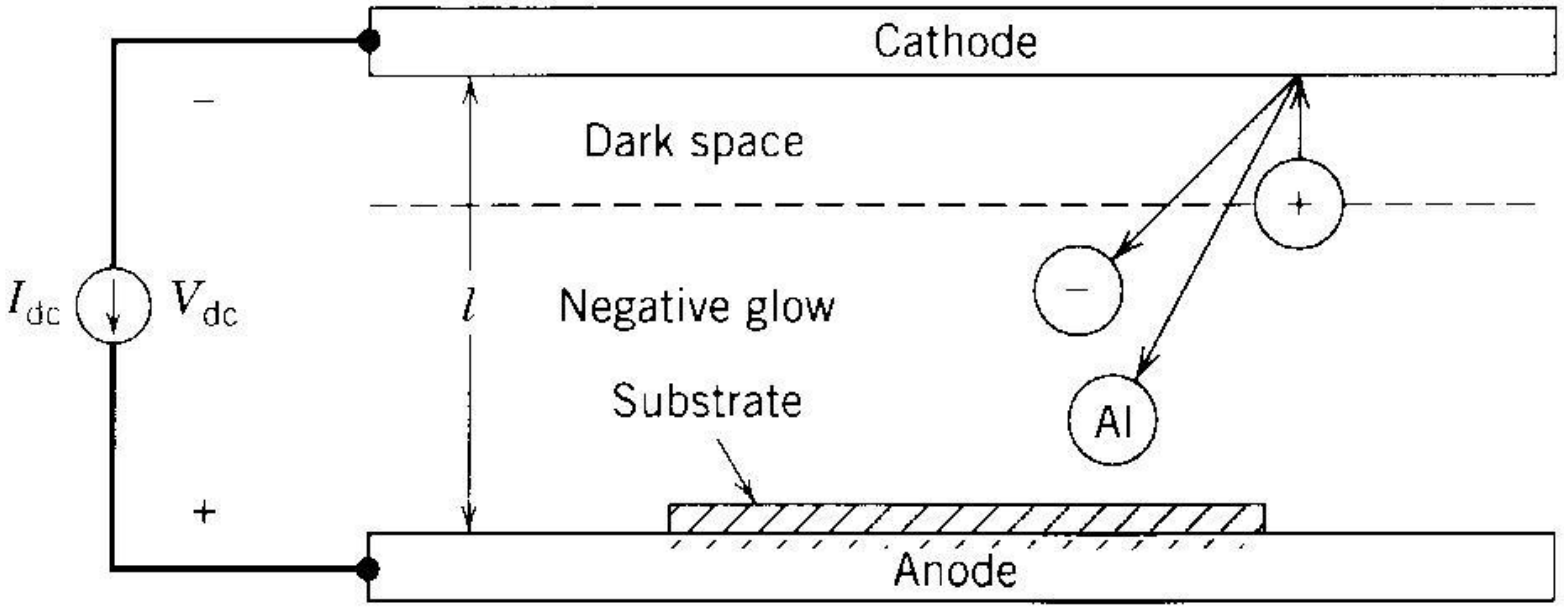

DC cathode sputtering- deposition of metallic thin films

-very old method used today only in very special cases of thin film deposition substituted recently by magnetron sputtering

disadvantage- limited deposition rate and impossible to use lower pressure than ≈4 –5 Pa

Fundamentals of sputtering and reactive sputtering process

The film deposition rate by sputtering:

$$D_{\text{sput}} = \frac{\gamma_{\text{sput}} \Gamma_i}{n_f} \frac{A_t}{A_s} \text{ cm/s}$$

Γ_i is the incident ion flux ($\text{cm}^{-2}\text{-s}^{-1}$), n_f the density of the deposited film (cm^{-3}), A_t (cm^2) is the target area sputtered, A_s (cm^2) is the substrate area on which the film is deposited, and γ_{sput} is the sputtering yield.

For energy of incident ions (500-1000 eV):

$$\gamma_{\text{sput}} \propto \frac{1}{\mathcal{E}_t} \frac{M_i}{M_i + M_t}$$

$\mathcal{E}_t$ is the surface binding energy of the target

M_i and M_t are the incident ion and target atom masses

Measured Sputtering Yields for Ar^+ at 600 V

Target	γ_{sput}
Al	0.83
Si	0.54
Fe	0.97
Co	0.99
Ni	1.34
Cu	2.00
Ge	0.82
W	0.32
Au	1.18
Al_2O_3	0.18
SiO_2	1.34
GaAs	0.9
SiC	1.8
SnO_2	0.96

Konuma, M. (1992), *Film Deposition by Plasma Techniques*, Springer, New York.

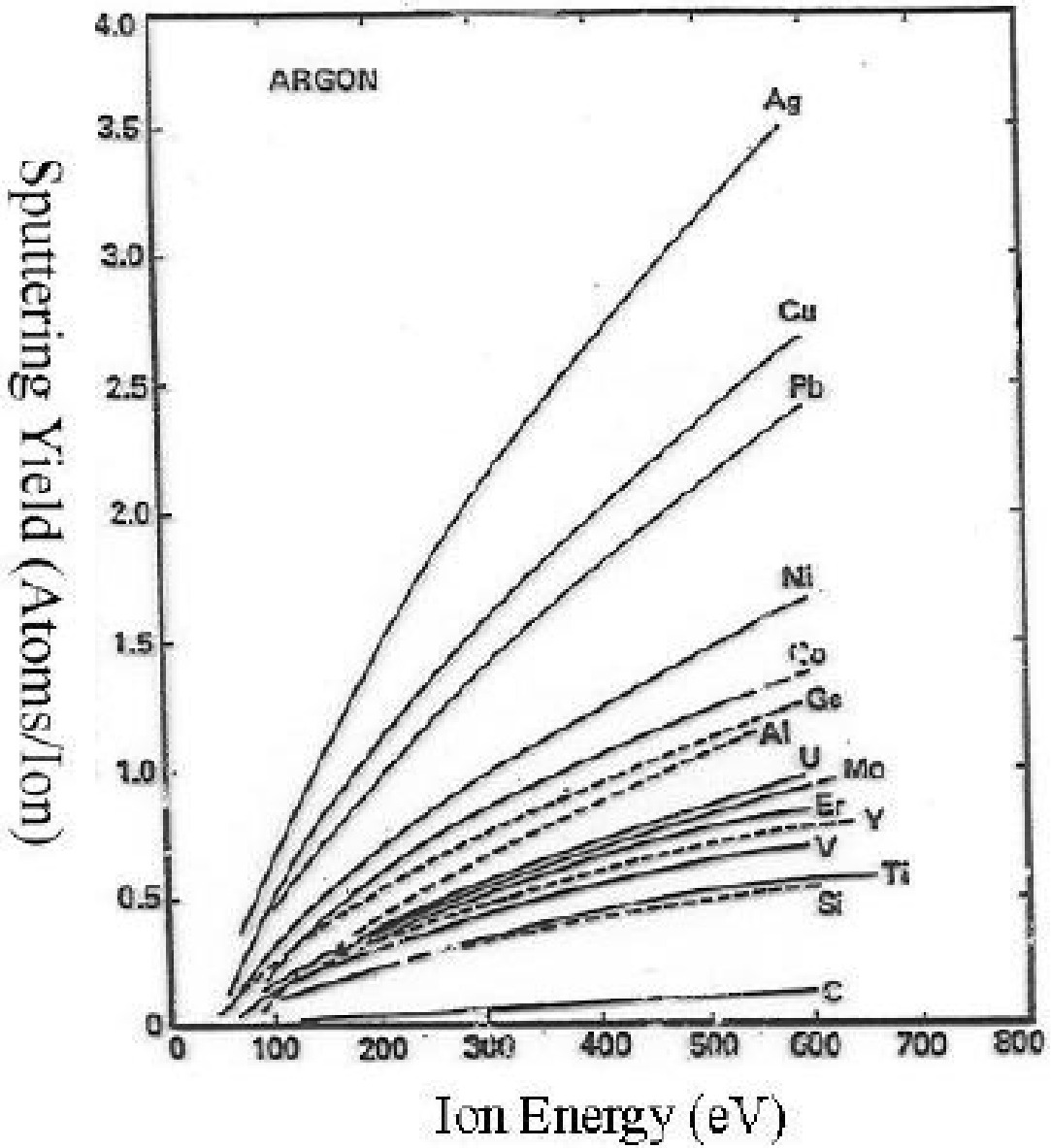

Sputter Yield (after Wehner)

Reactive sputtering:
reactive gas is added in to discharge in order to
react with sputtered particles (usually on the substrate) or with the target surface
examples
deposition of AlN with Al cathode and Ar+N_2 gas
deposition of SiO_2 with Si cathode and Ar+O_2 gasses
deposition of TiO_2 with Ti cathode and Ar+O_2 gasses
deposition of Al_2O_3 with Al cathode and Ar+O_2 gasses

metallic mode: target is not poisoned by reaction with reactive gas (for example by SiO_2 or TiO_2)- original material of the target (Si or Ti) are sputtered a react with reactive gas on the substrate

reactive mode: Target is covered by (SiO_2 or TiO_2) during process and these oxides are sputtered from the target $\Rightarrow$ possible undesirable arcing (in DC sputtering)

Some problems were overcome by increasing plasma density in front of the substrate ⇒ lower operating pressure, higher sputtering rate and many other advantages

The most wide system used is planar magnetron sputtering system:

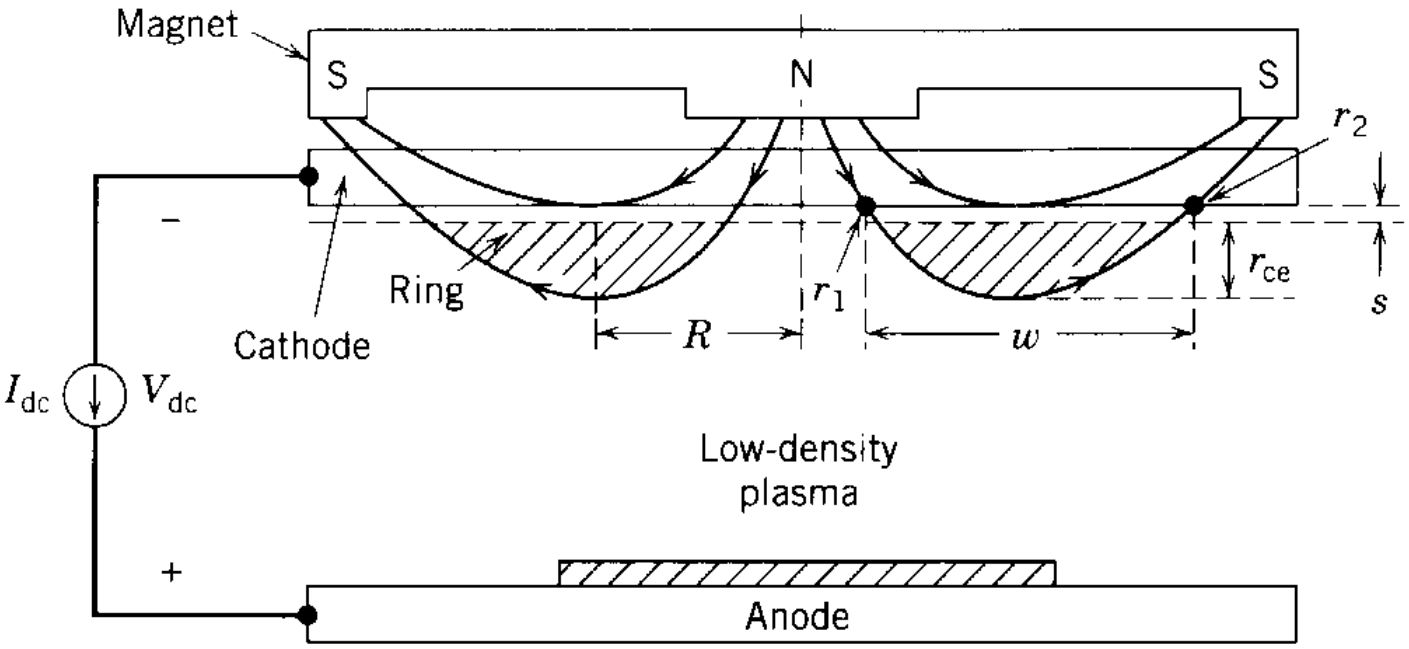

DC magnetron

Principle of a Magnetron Discharge

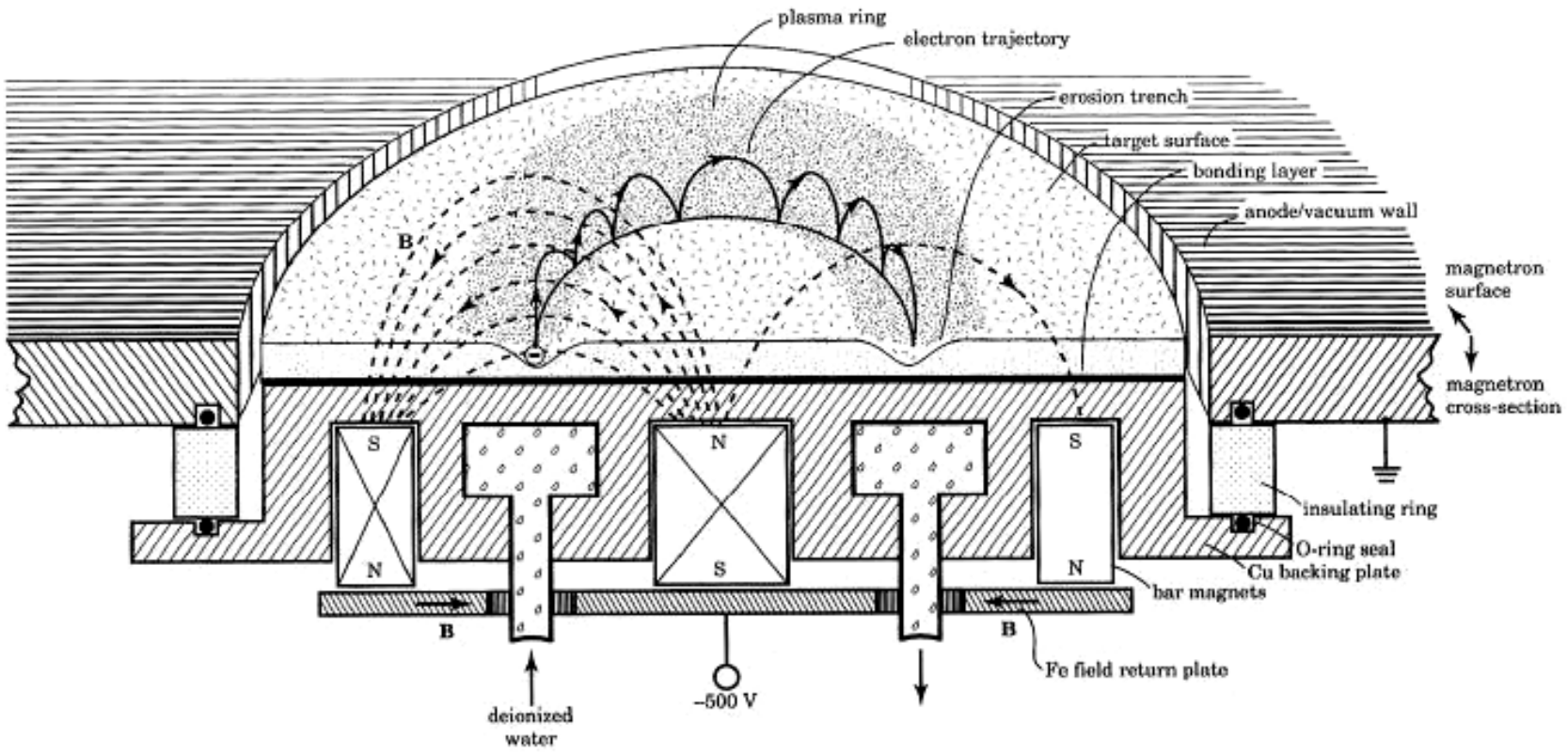

Scheme of a circular planar magnetron according to Smith. The magnetic field is depicted as dashed lines, while the cycloidal electron path is shown in larger size for clarity.

R. Hippler, H. Kersten, M. Schmidt, K.H. Schoenbach (Eds.), **Low Temperature Plasmas Fundamentals, Technologies, and Techniques,** WILEY-VCH Verlag Berlin GmbH 5th June 2007

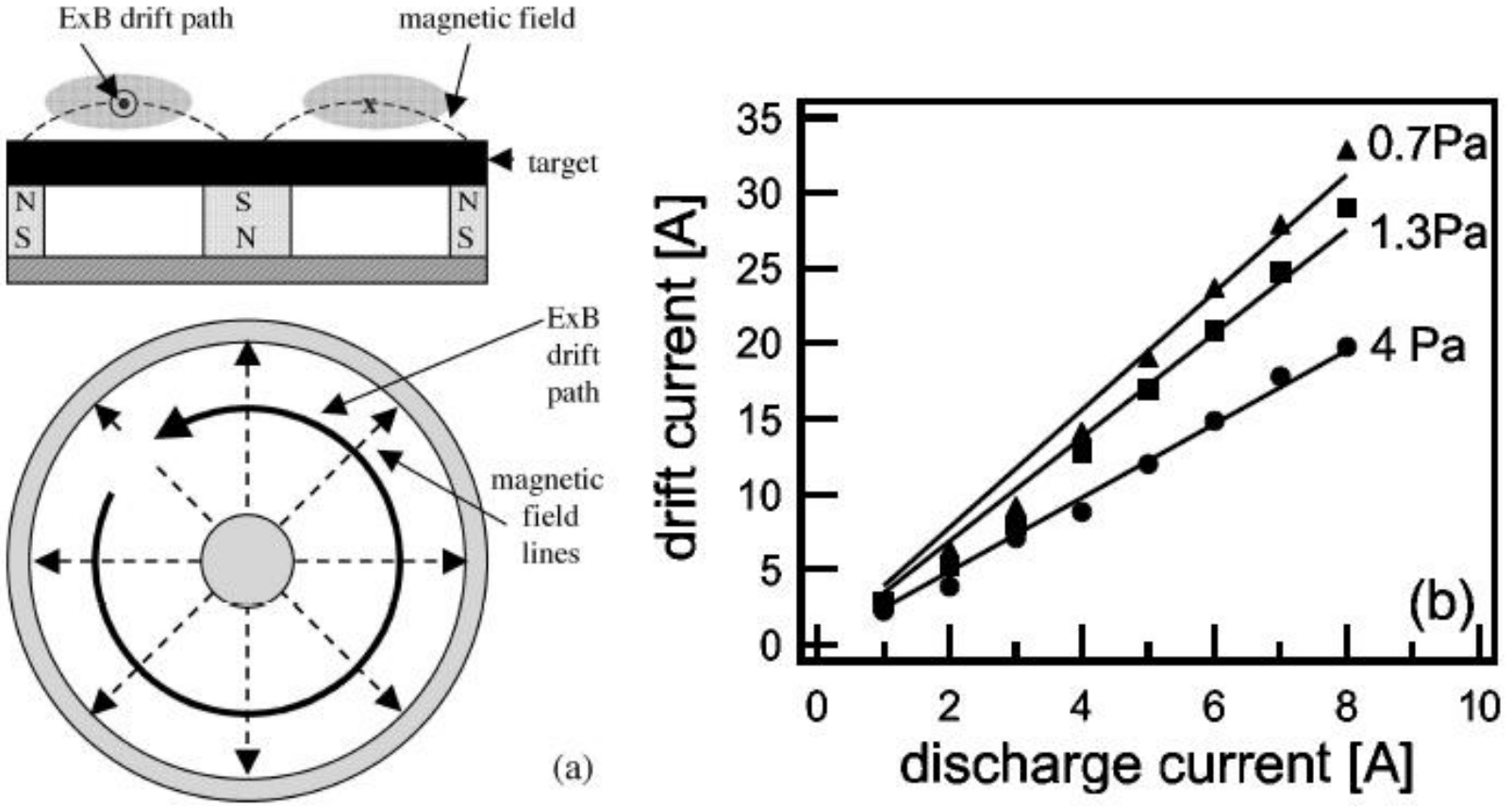

(a) Top and side view of a planar circular magnetron, the schematic magnetic and electric field and the resulting $\vec{E} \times \vec{B}$ drift path (after Rossnagel and Kaufman [50]). (b) Measured total drift currents as a function of the discharge current at different working pressures in an argon discharge with a copper target [49].

R. Hippler, H. Kersten, M. Schmidt, K.H. Schoenbach (Eds.), **Low Temperature Plasmas Fundamentals, Technologies, and Techniques,** WILEY-VCH Verlag Berlin GmbH 5th June 2007

Typical conditions for DC magnetron sputtering

- $B_0 \sim 200$ G
- $p \sim 2$–5 mTorr argon
- $\bar{J}_i \sim 20$ mA/cm^2
- $V_{dc} \sim 600$ V
- Deposition rate ~ 2000 Å/min

Here B_0 is the magnetic field strength at the radius R where the magnetic field line is tangential to the cathode surface, and $\bar{J}_i$ is the average ion current density over the ring area.

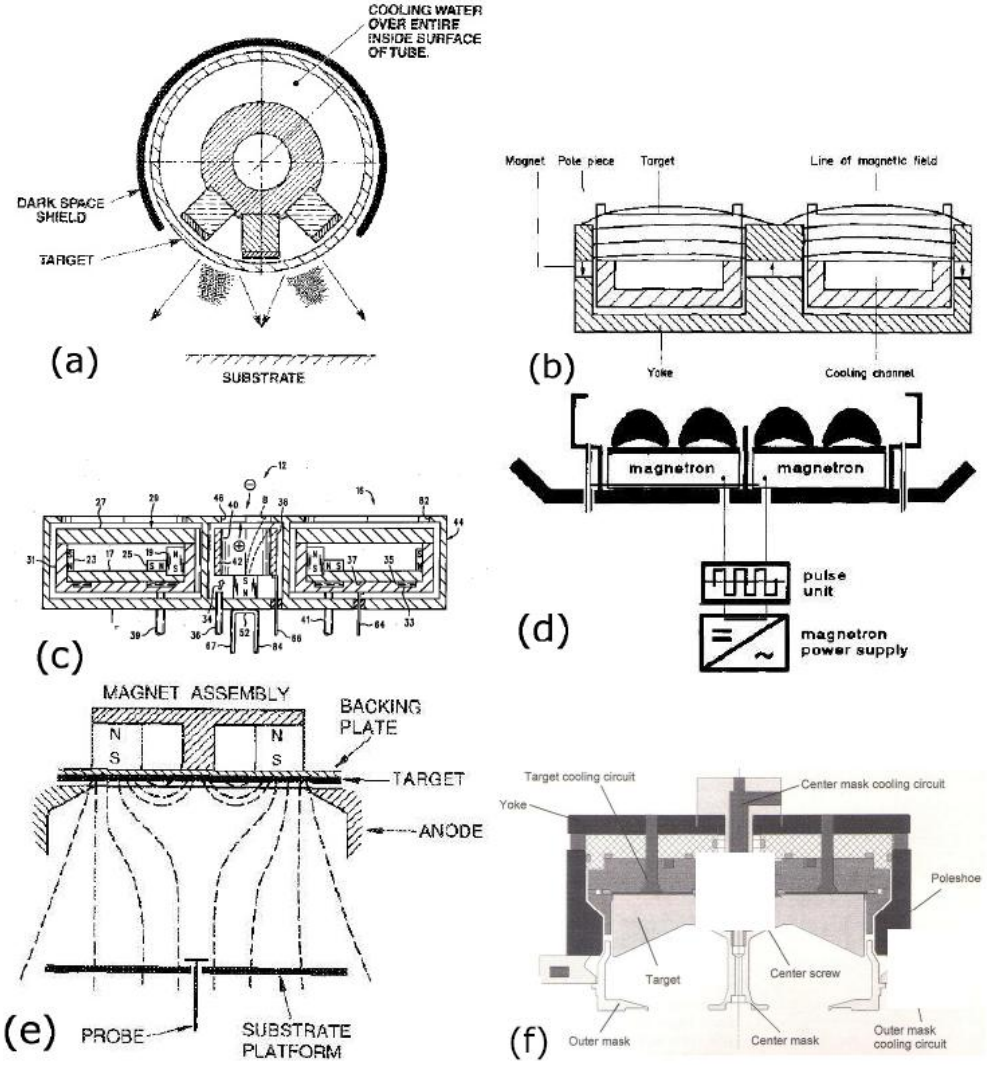

Layout of selected modern magnetron sputtering sources: (a) Rotatable cylindrical magnetron (Wright and Beardow (1986) [56]), (b) Interpole magnetron (Kukla (1990) [35]), (c) ciruclar magnetron with inserted hollow cathode electron source (Manley (1998) [65]), (d) dual magnetron with bipolar-pulsed power supply [62], (e) unbalanced magnetron (Window and Savvides (1986) [60]), (f) CD metallization magnetron source (Singulus II, Lübbehusen et al. (1995) [64]).

IPVD magnetron system with additional ICP RF discharge - ICP MS

It makes possible to improve properties of metal films in microelectronics as Al, Cu etc.
It can improve hard coatings as TiN, etc.
Ionized particle is easy to control by electric or magnetic field
The films can be deposited on substrates with trenches.

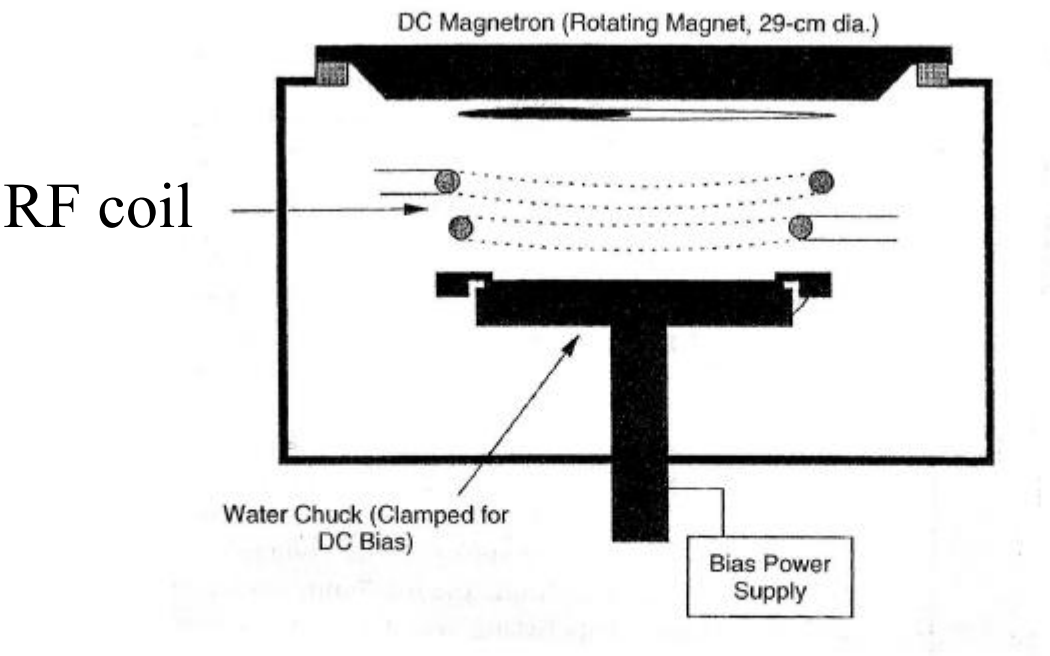

Figure 25.15: Scheme of a manufacturing ionized-sputtering tool for the deposition of metal films in microelectronics.

Ion density in ICP-MS versus applied RF power in ICP-MS.

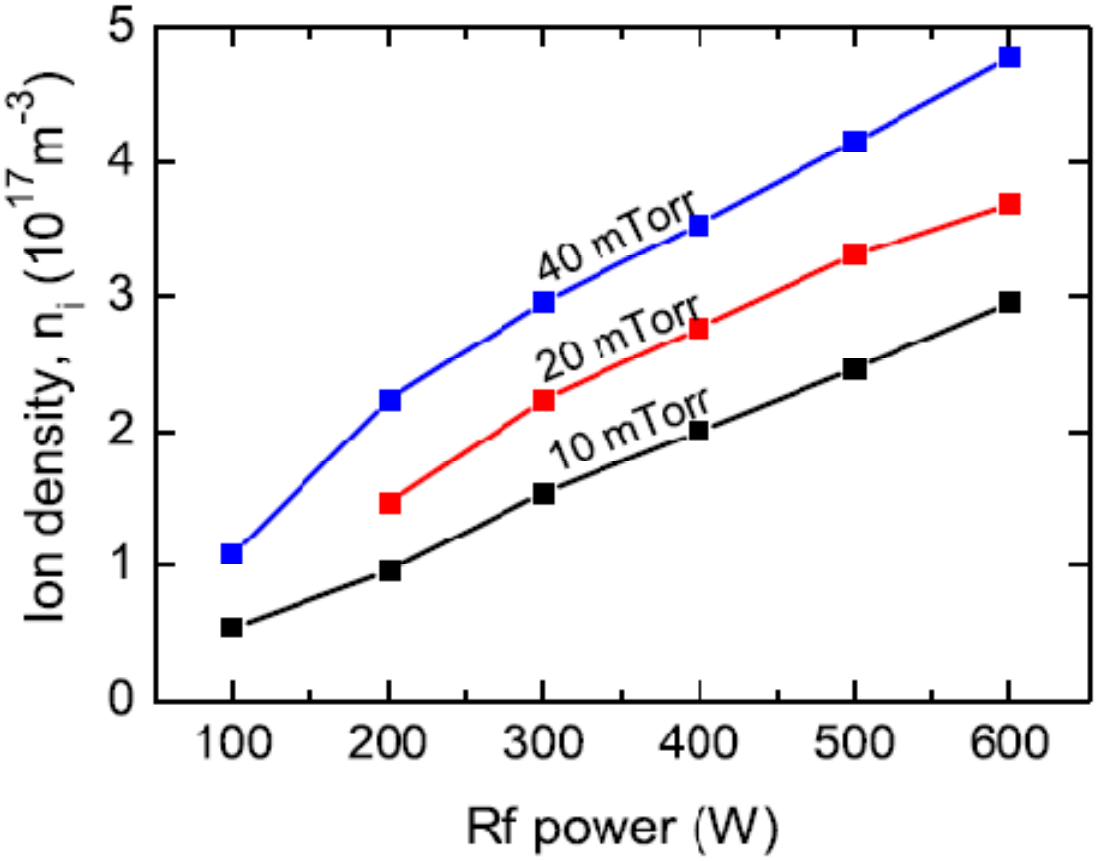

Fig. 3. The ion density versus applied rf power for an ICP-MS Ar discharge at different pressures (from Wang et al. [49]).

Degree of ionization of sputtered Cu in ICP-MS

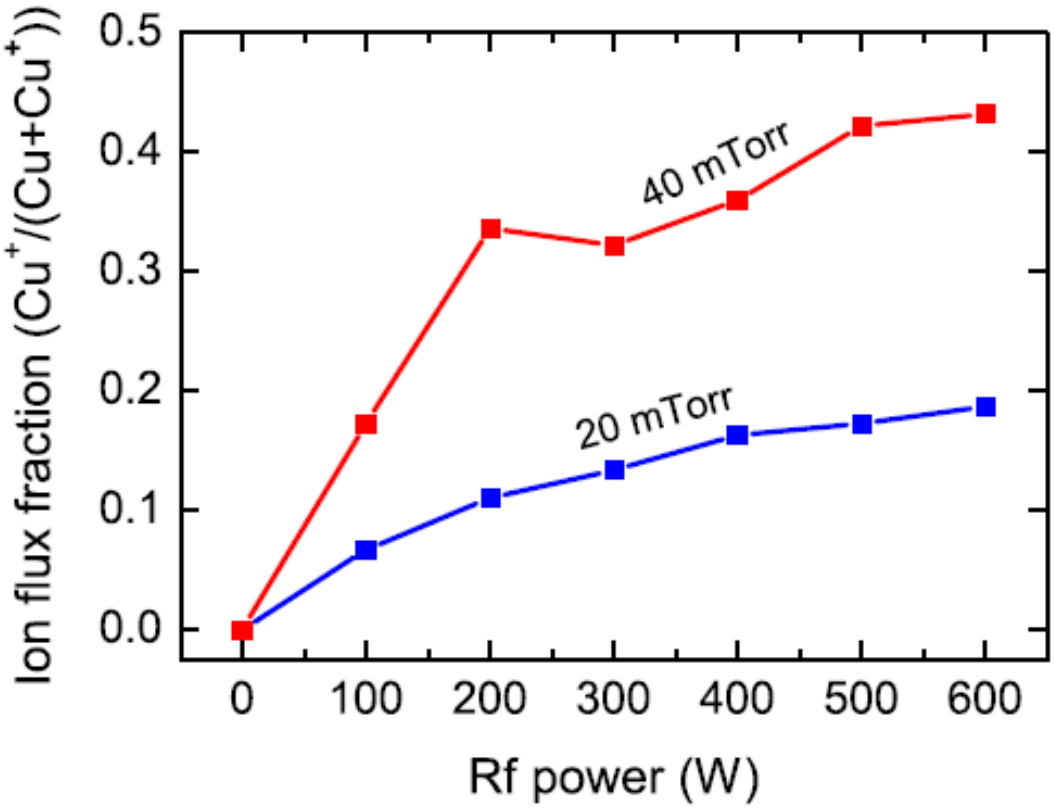

Fig. 4. The ionized fraction of sputtered Cu versus applied rf power for an ICP-MS Ar discharge at 20 and 40 mTorr (from Wang et al. [49]).

RF sputtering fundamentals

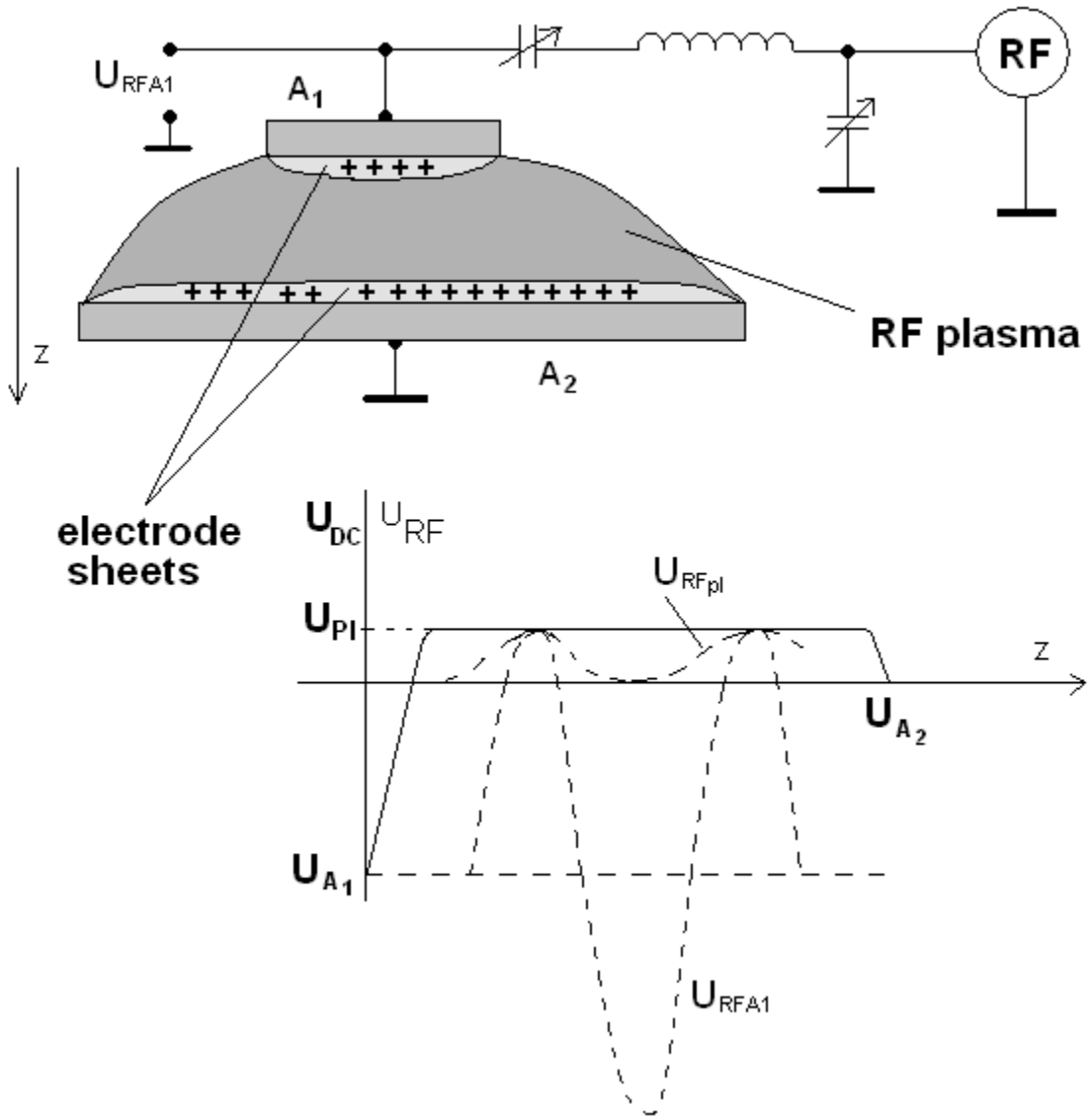

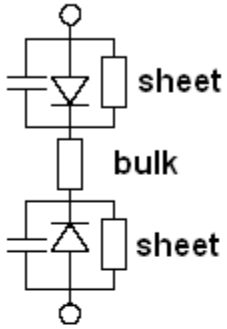

equivalent discharge circuit

RF sputtering advantages:

-Electrodes (active electrode) can be fully covered by thick dielectric target which will be sputtered (for example Er_2O_3, Y_2O_3, SiO_2 , TiO_2, Al_2O_3 targets
-suppressed arcing

RF sputtering disadvantages:

more technically difficult
RF interference
limited size of target, etc..

RF magnetron sputtering (possible dielectric target)

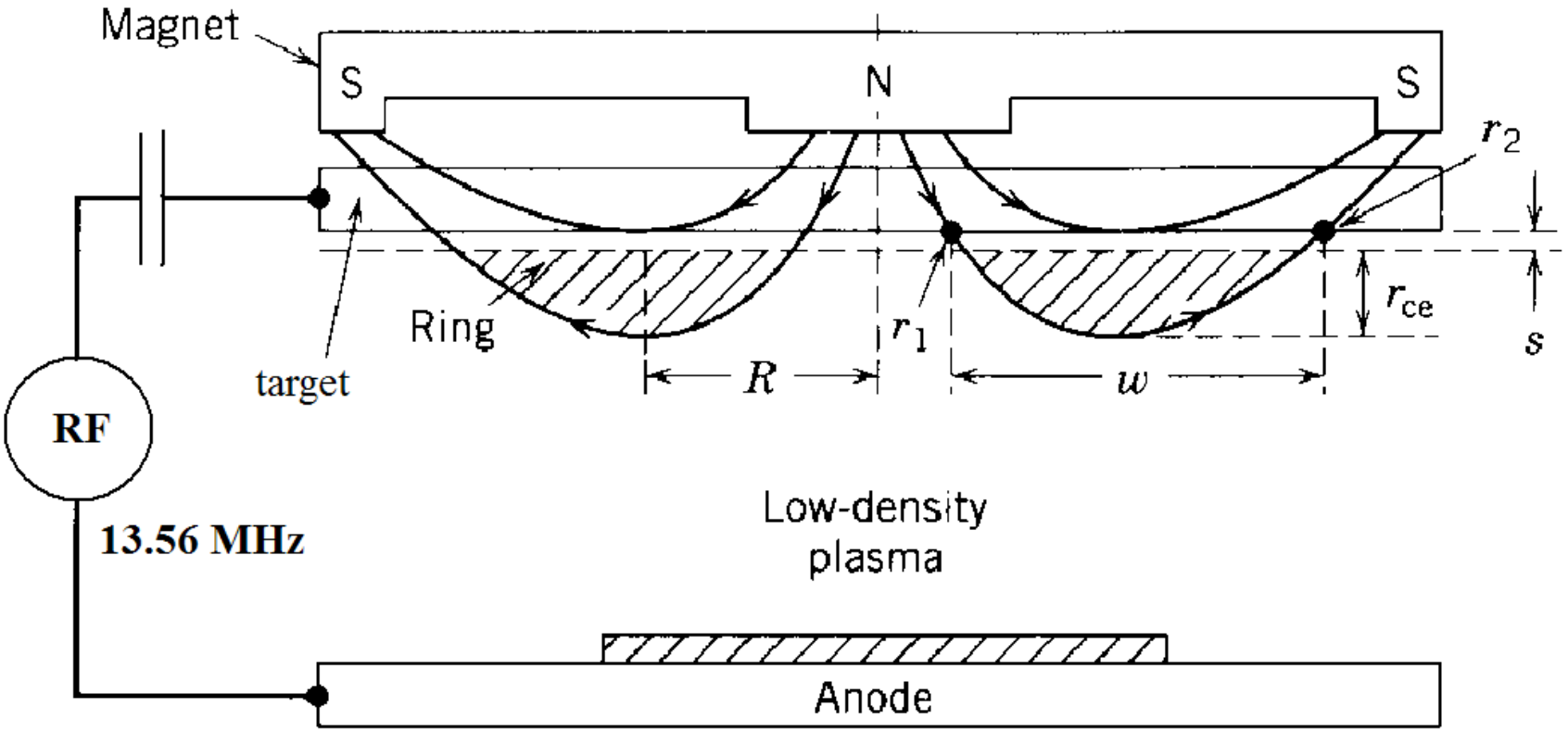

DC pulsed reactive sputtering of TiO_2 thin films

Ti target, Ar + O_2 gas mixture

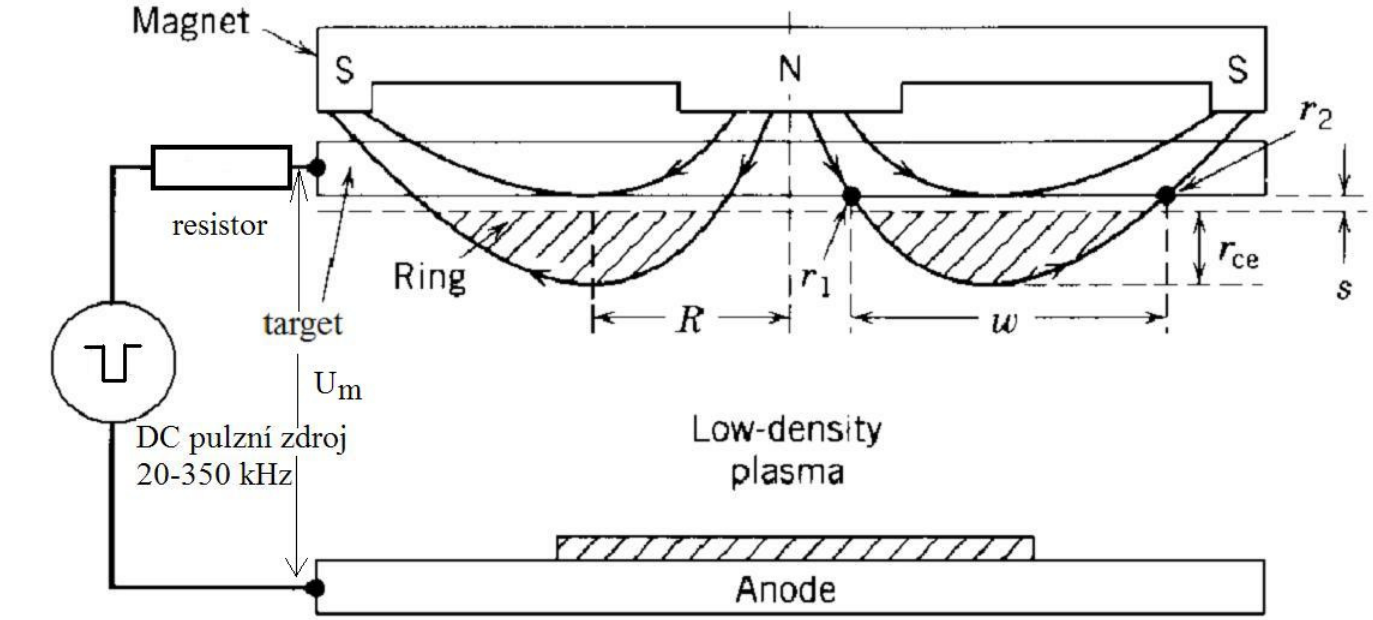

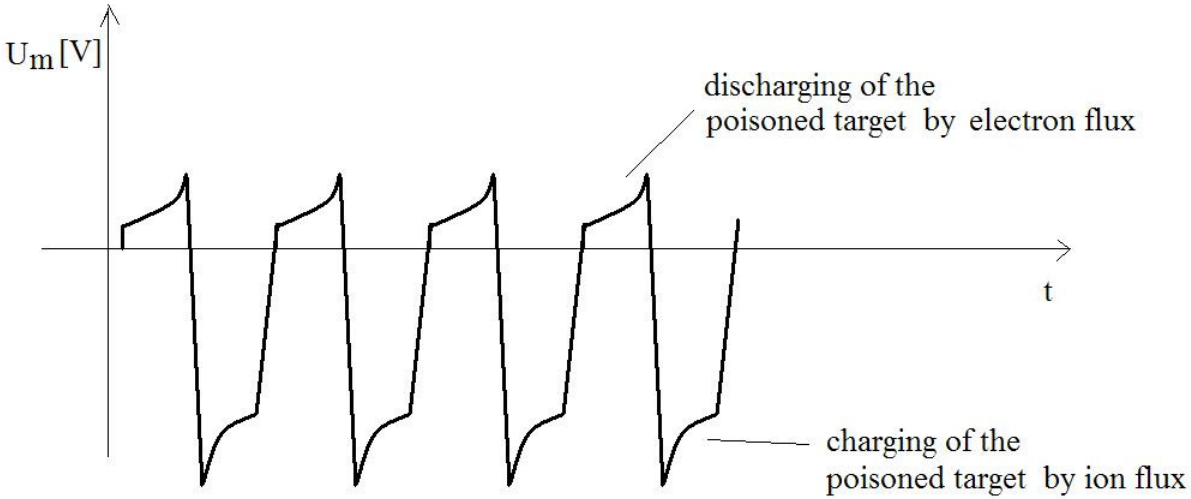

Advantages of DC pulsed sputtering MS (20-350 kHz) for reactive sputtering of metal target in Ar+O_2 gas mixture:

-suppressing arcing of the oxidized target

-increasing of plasma density, increasing of ion flux and heating flux on the substrate $\Rightarrow$ higher quality of deposited oxide thin films (TiO_2, ZnO, Al_2O_3). The films have higher density, better adhesion and lower

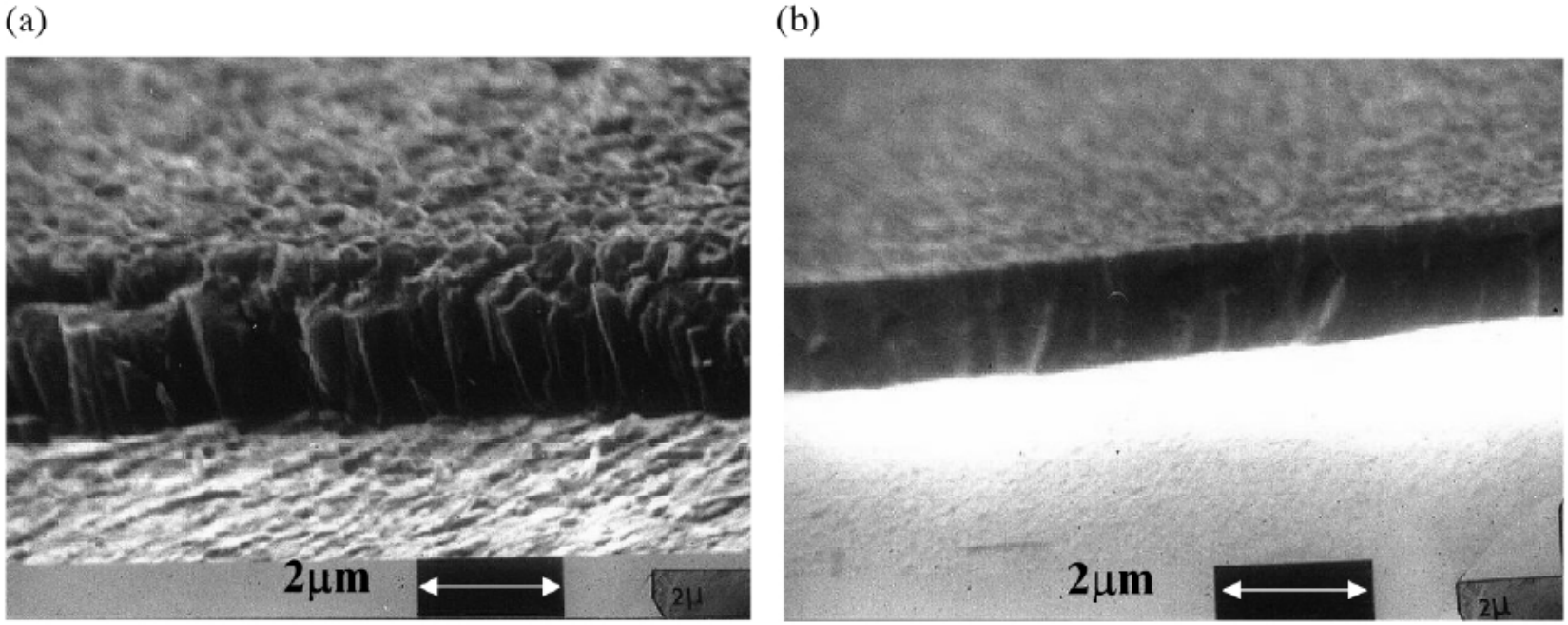

Fig. 1. SEM micrographs of the fracture sections of titania coatings deposited onto glass substrates by (a) continuous and (b) pulsed DC reactive magnetron sputtering. Target current, 6 A; pressure, 2×10^{-3} mbar; floating bias.

HIPIMS High power impulse magnetron sputtering

high power in pulse and low mean power

$n_e \approx 10^{19}\ m^{-3}$

major fraction of sputtered atoms are ionized

lower porosity and higher density of deposited films (CrN)

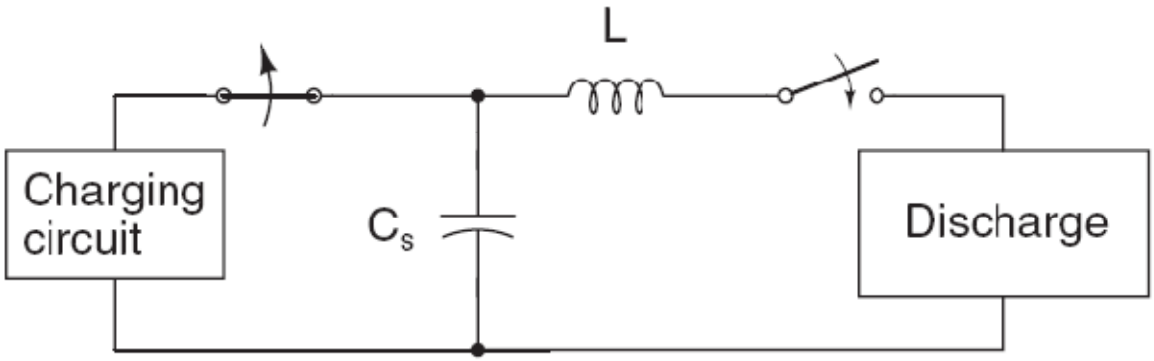

Fig. 8. The basic single-mesh *LC* network between the charging HIPIMS power supply and the discharge load.

A.P. Ehiasarian, R. New, W.-D. Münz, L. Hultman, U. Helmersson, V. Kouznetsov, Vacuum 65 (2002) 147.

Example of DC pulsed magnetron in HIPIMS mode

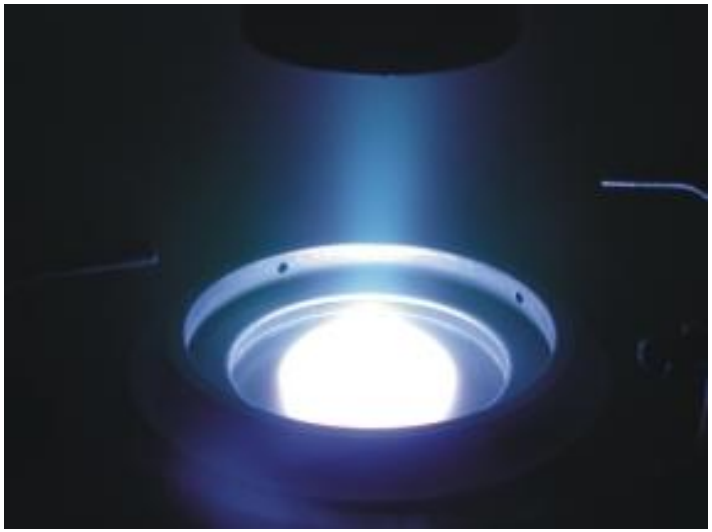

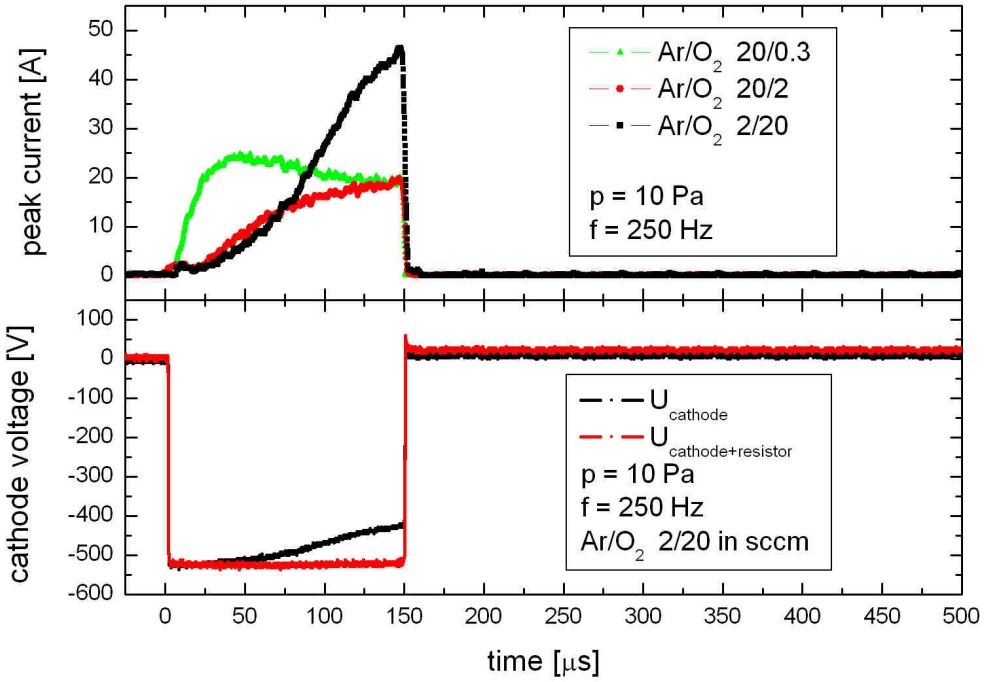

HIPIMS and dc- magnetron sputtering

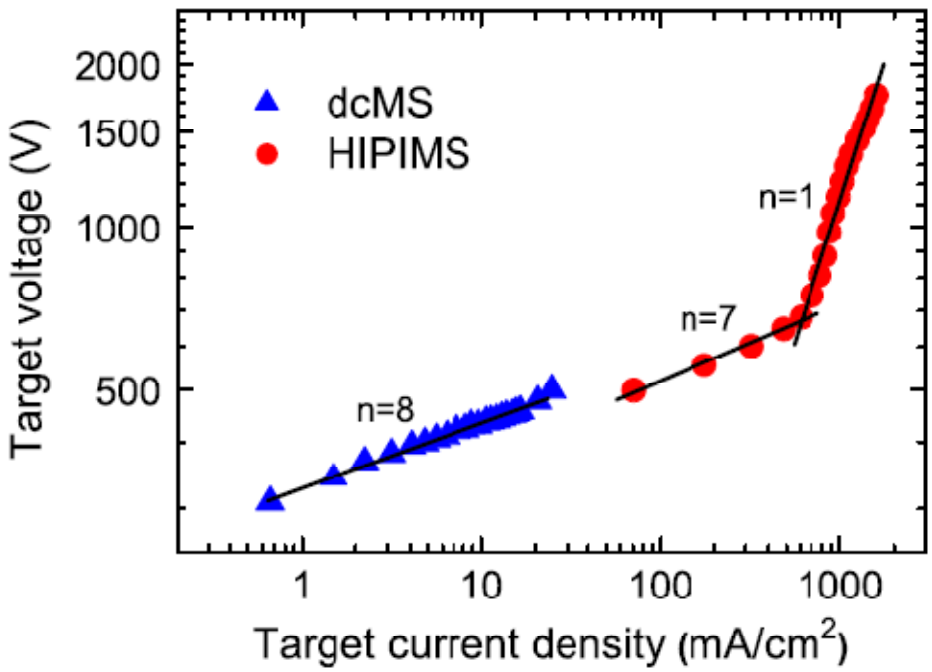

Fig. 11. The target voltage versus the target current density for a conventional dcMS discharge and a HIPIMS discharge. The exponent n of the power law $I_d = k_d V_d^n$ is indicated. The target is Cr and the Ar pressure is 3 mTorr (from

A.P. Ehiasarian, R. New, W.-D. Münz, L. Hultman, U. Helmersson, V. Kouznetsov, Vacuum 65 (2002) 147.

Electron density evolution in HIPIMS system

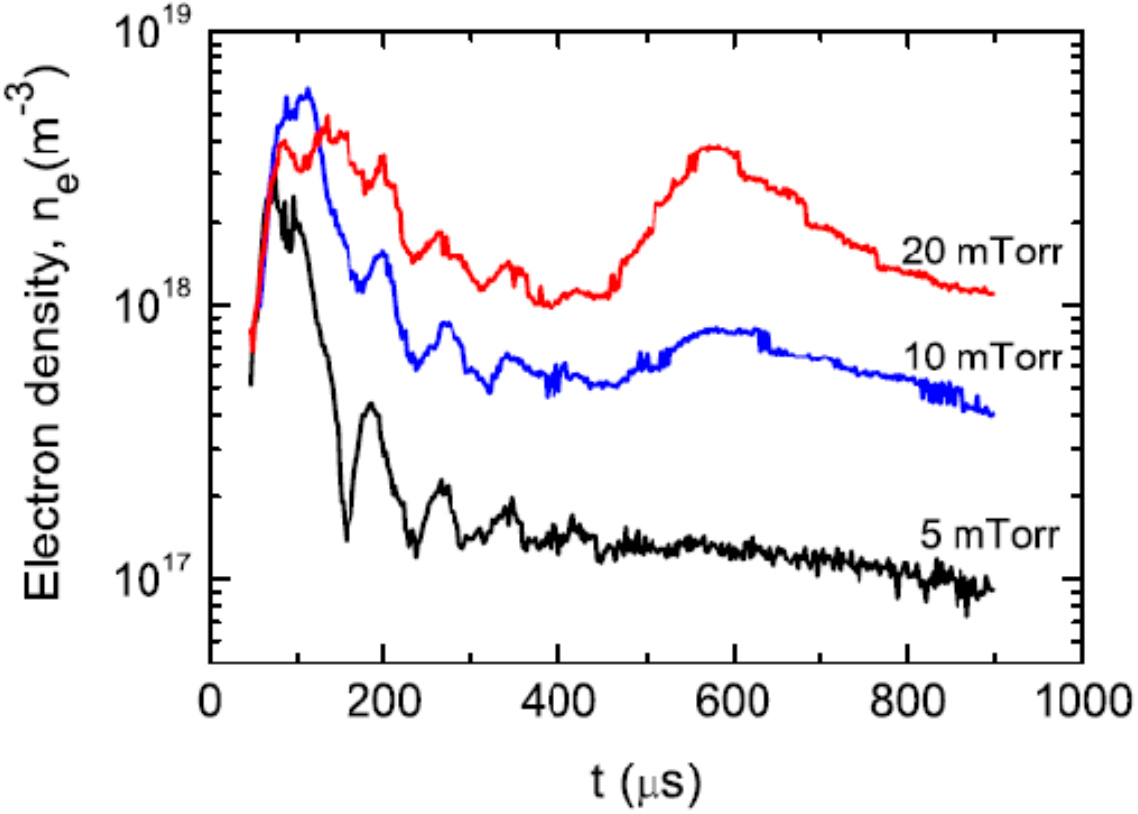

Fig. 12. The electron density as a function of time following HIPIMS pulse initiation at different Ar pressures from (Gudmundsson et al. [74]).

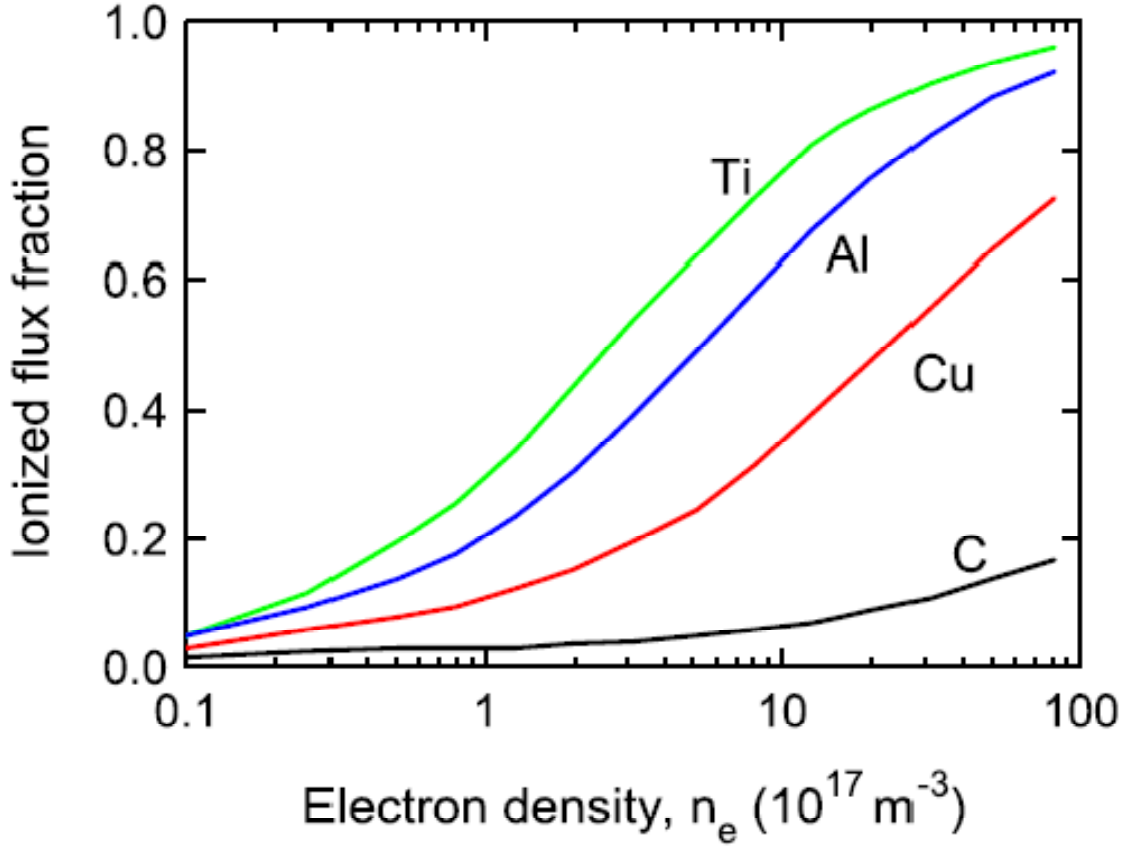

Fig. 1. The ionized flux fraction of the sputtered material as a function of the electron density as modeled by Hopwood [2].

[2] J.A. Hopwood, in: J.A. Hopwood (Ed.), Thin Films: Ionized Physical Vapor Deposition, Academic Press, San Diego, 2000, p. 181.

Example of sputtered Ti atoms ionization in HIPIMS

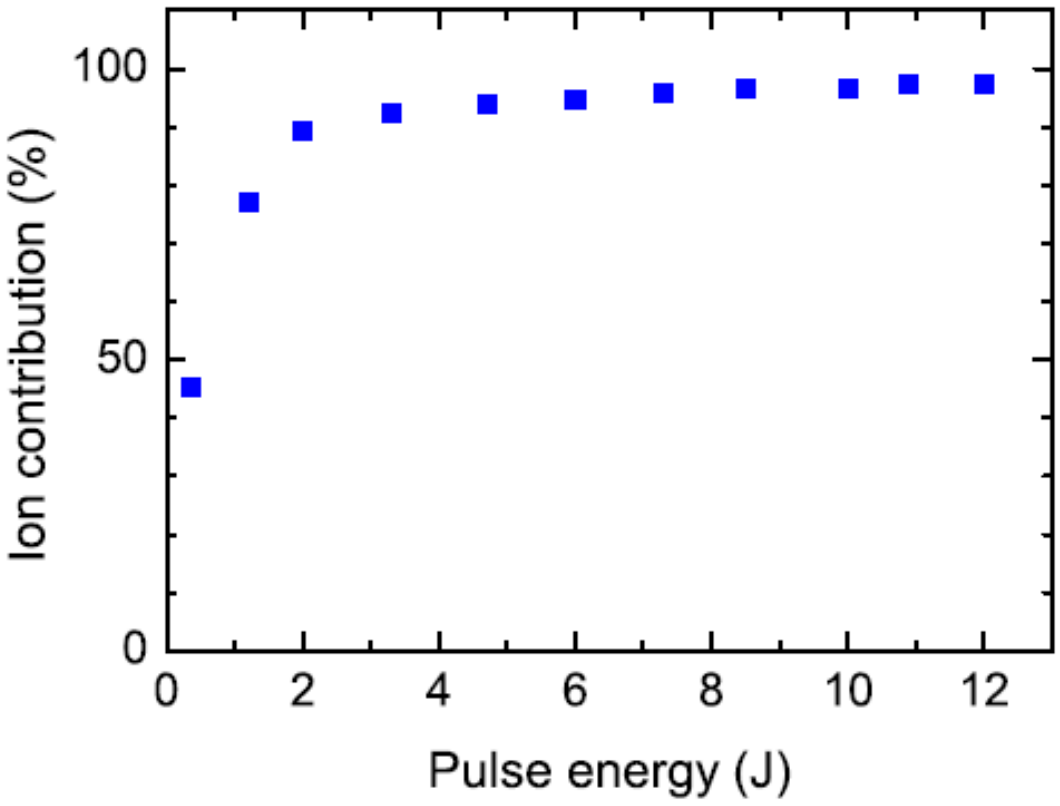

Fig. 21. The fractional Ti^+ contribution of the sputtered Ti as a function of applied HIPIMS pulse energy calculated from optical emission spectra (from Bohlmark et al. [64]).

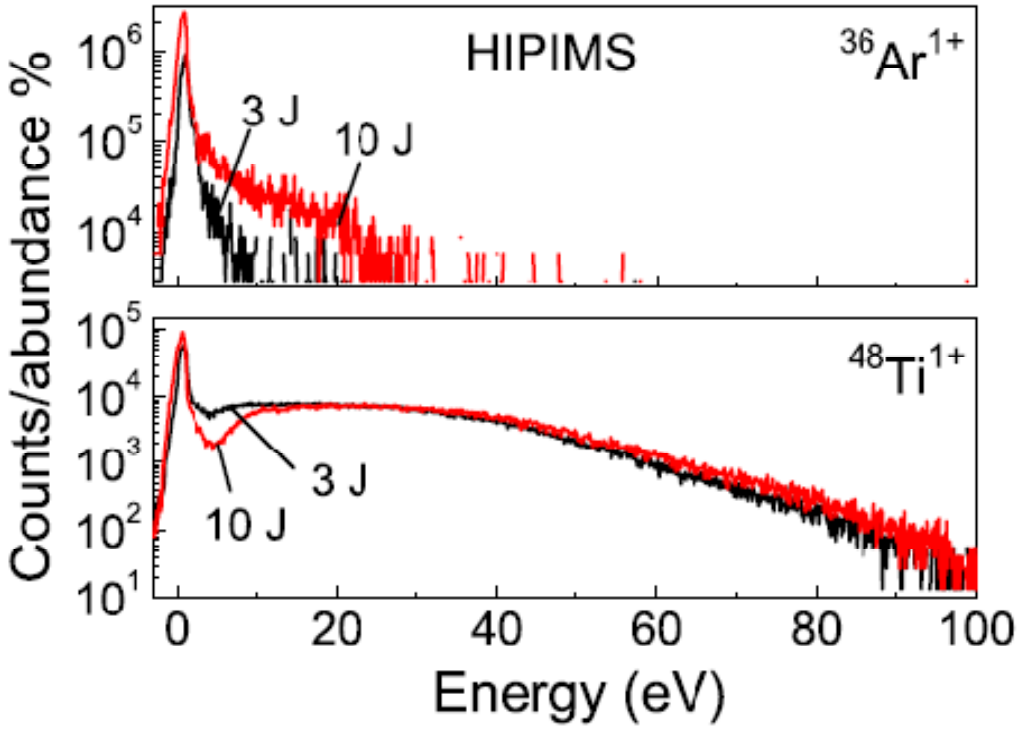

Fig. 17. The energy distributions of Ar^+ and Ti^+ in a HIPIMS discharge with two different pulse energies at an Ar pressure of 3 mTorr (from Bohlmark et al. [88]).

[88] J. Bohlmark, M. Lattemann, J.T. Gudmundsson, A.P. Ehiasarian, Y.A. Gonzalvo, N. Brenning, U. Helmersson, Thin Solid Films (in press).

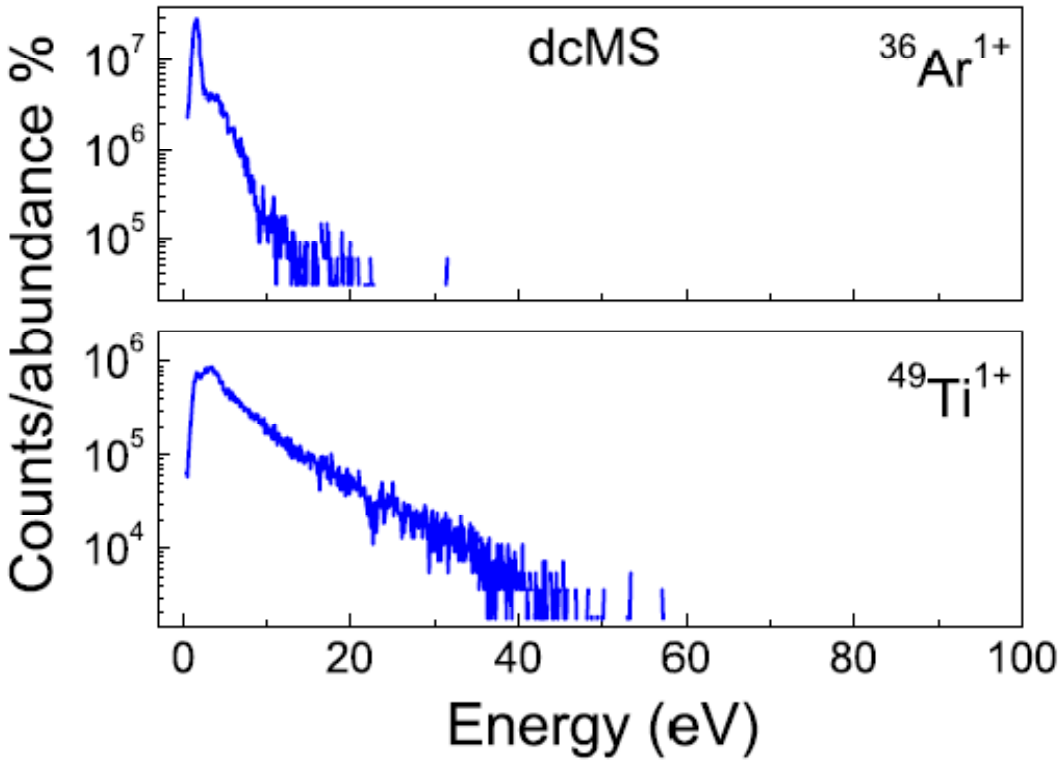

Fig. 18. The energy distribution for Ar^+ and Ti^+ ions in a conventional dcMS discharge (from Bohlmark et al. [88]).

[88] J. Bohlmark, M. Lattemann, J.T. Gudmundsson, A.P. Ehiasarian, Y.A. Gonzalvo, N. Brenning, U. Helmersson, Thin Solid Films (in press).

Comparison of deposition rates for dcMS and HIPIMS

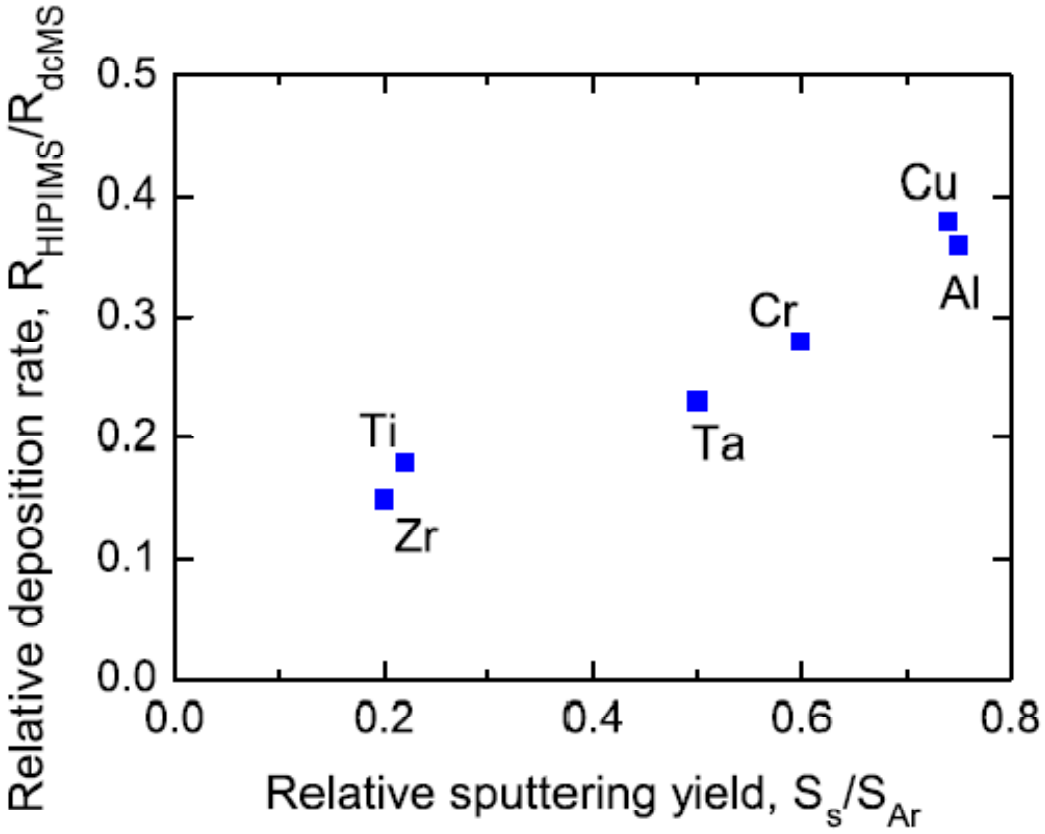

Fig. 23. Deposition efficiency for HIPIMS and conventional dcMS plotted for several metal targets: relative deposition rate vs. self-sputtering yield S_S divided with its Ar-sputter yield S_{Ar} (from Helmersson et al. [67]).

Deposition of Ta films by HIPIMS and dcMS into deep trench

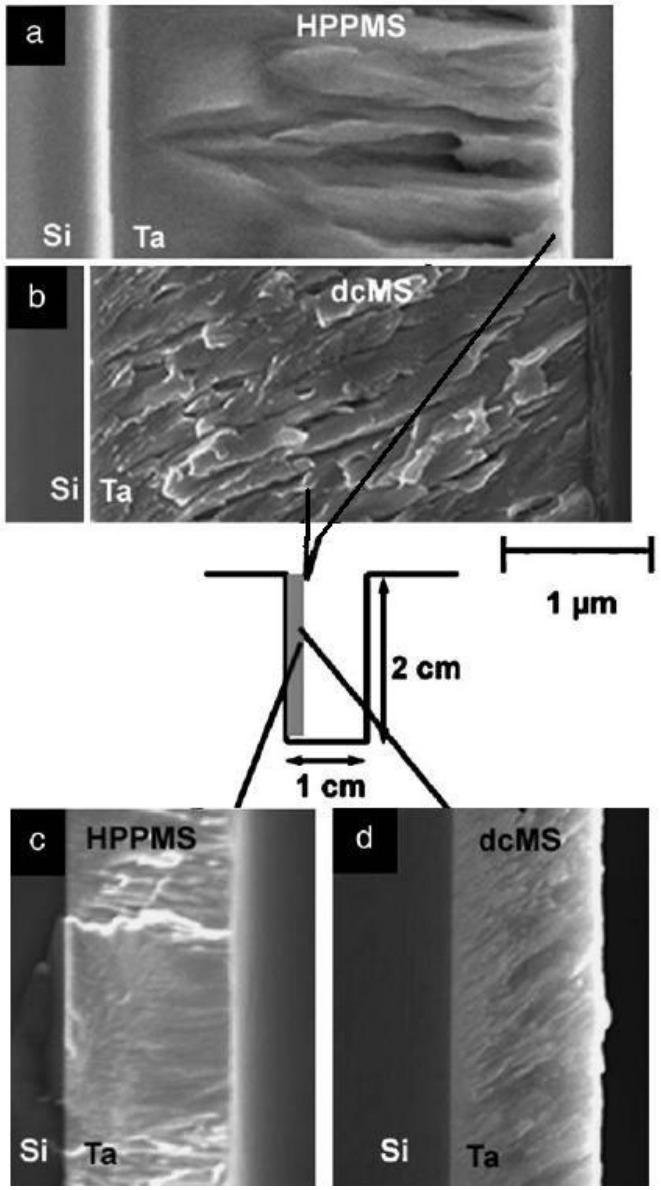

SEM images of Ta films grown by HIPIMS and dcMS near the opening of a 1 cm wide by 2 cm deep trench (a) and (b), and approximately half way down the wall of the trench (c) and (d). Both films were grown at room temperature with a substrate bias of −50 V (from Alami et al. [7]).

Application of RF magnetron sputtering on Er_2O_3, Y_2O_3 as barrier insulating coatings in fusion devices

Akihiko Sawada Fusion Engineering and Design 75–79 (2005) 737–740

-the target used was made of Y_2O_3 or Er_2O_3 bulk,

- substrates of SUS430, vanadium metal or V–4Cr–4Ti alloy (named NIFS Heat II)

- Ar gas was used

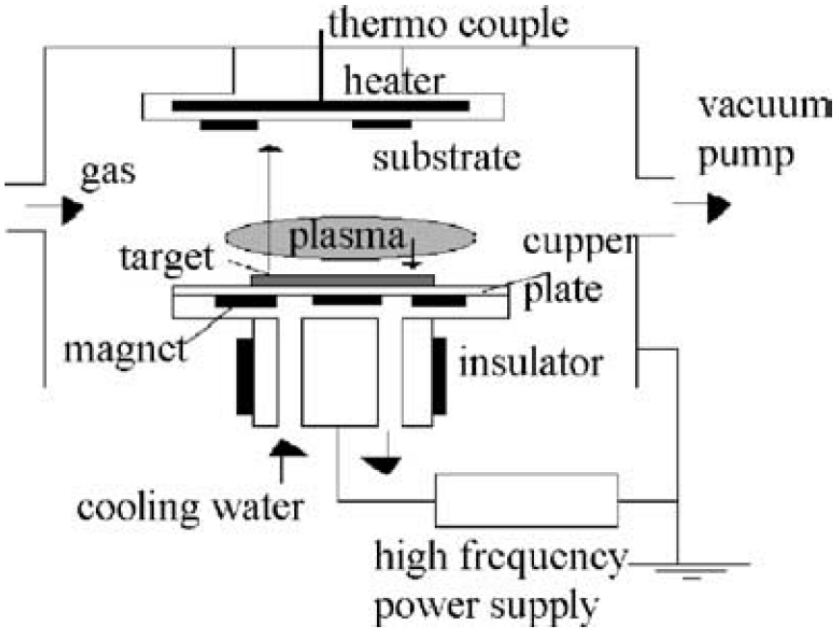

Fig. 1. Fabrication apparatus for RF sputtering method.

Akihiko Sawada Fusion Engineering and Design 75–79 (2005) 737–740

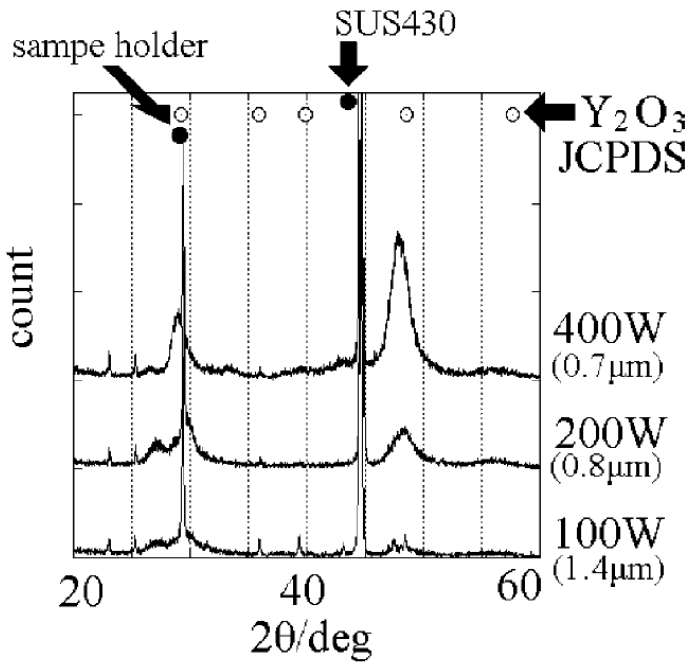

Fig. 3. Difference in XRD patterns of Y_2O_3 coatings fabricated by RF sputtering with three different electrical powers on SUS430.

resistances of Y_2O_3 and Er_2O_3 deposited films were 10^{12} –10^{14} Ωm as required in fusion device.

Cathodic arc plasma deposition

-A cathode arc, vacuum arc, or metal-vapor arc is an arc that passes current between electrodes by means of vaporized electrode material of the arc itself.

-It can work in vacuum without noble gas as argon

- Arc discharges are characterized with high currents in the range from the lower threshold current (the chopping current) of approximately 30 A up to kA. The discharge runs at a low voltage in the range typically 20–100 V.

-The current in a vacuum arc discharge is often concentrated in a luminous area of a few square micrometers on the cathode termed the cathode spot.

-The time scale of ignition and explosion of the spot are 1–10 ns and its residence time is of the order of 100 ns.

-The plasma density in the cathode spots is of the order of 10^{26} m^{-3} and the current density is as high as 10^{12} Am^{-2} .

-When the current reaches a threshold of approximately 150 A, a second

The CAPD method is characterized by the following:

(1) The very high percentage of the emitted vapor that is ionized, 30–100%;
(2) The emission of ions that are multiply charged; and
(3) The high kinetic energy of the emitted ions, 10–100 eV.

These characteristics yield the following benefits in coating quality and process control:

(1) High film adhesion and density;
(2) High deposition rates with excellent coating uniformity;

(3) High-quality, stoichiometric reacted coatings over a wide range of processing conditions;
(4) Low substrate temperatures during deposition; and
(5) Retention of alloy composition from target to deposited film.

Basic cathodic arc plasma deposition system

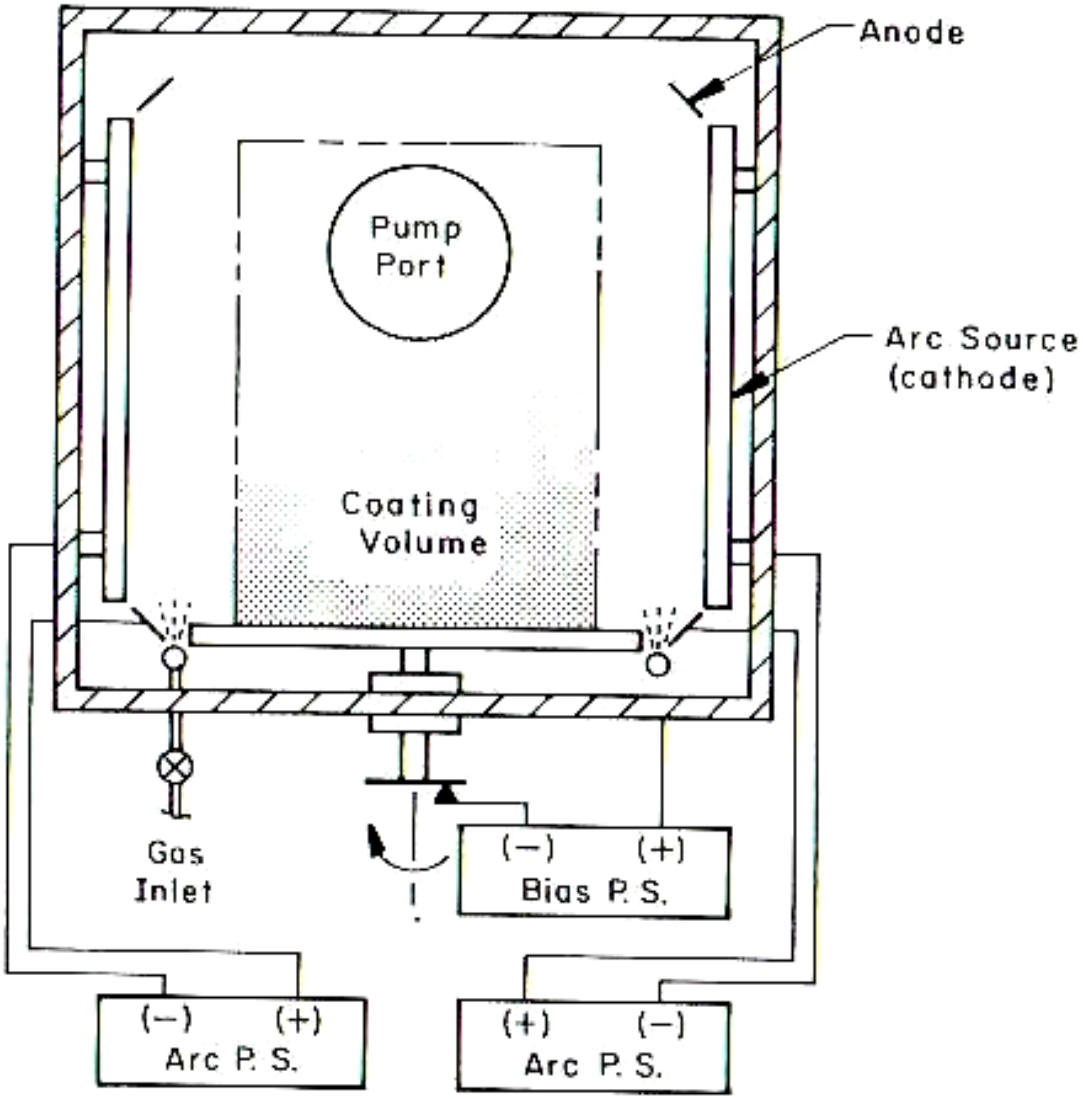

Fig. 1. A basic CAPD coating system.

Detail of cathode spot

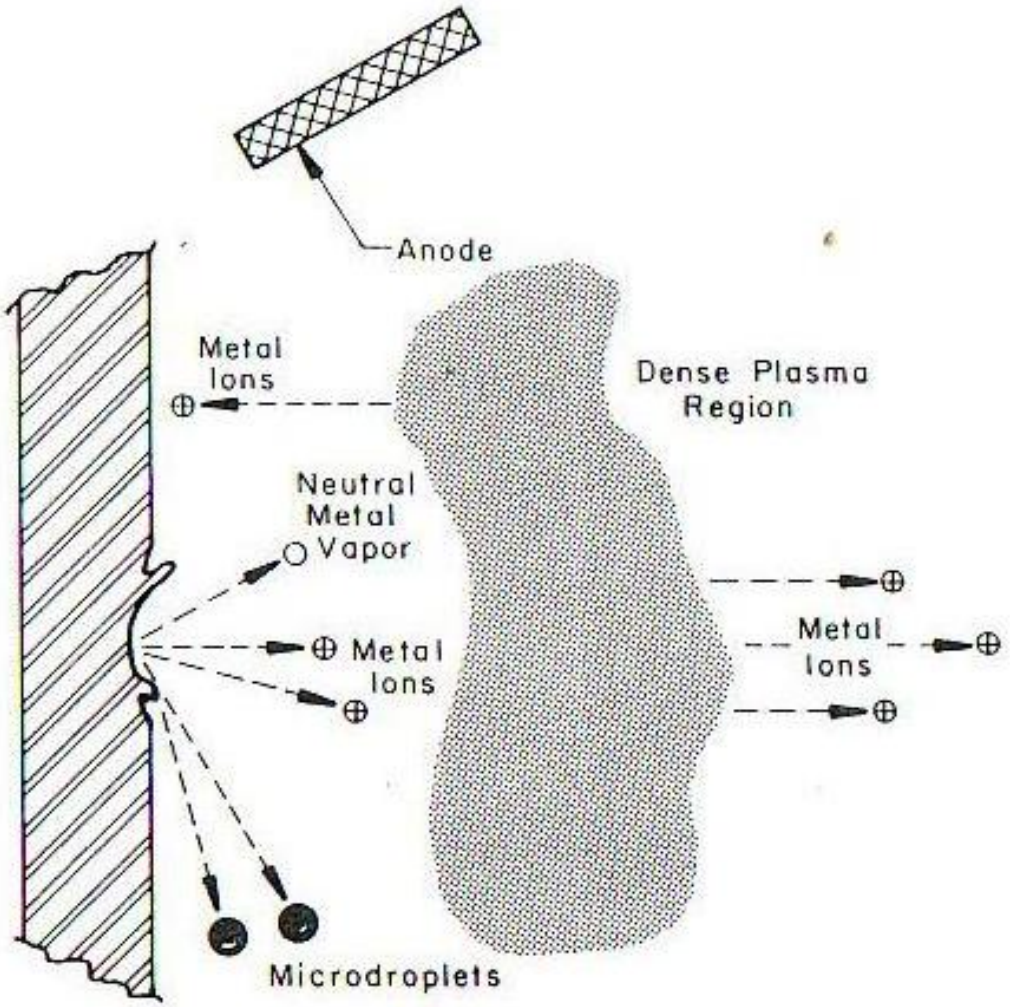

Fig. 13. Cathode spot region of a vacuum arc.

Bombardment of the substrate (ion plating) by DC voltage applied on the space charge sheet existing around the surface

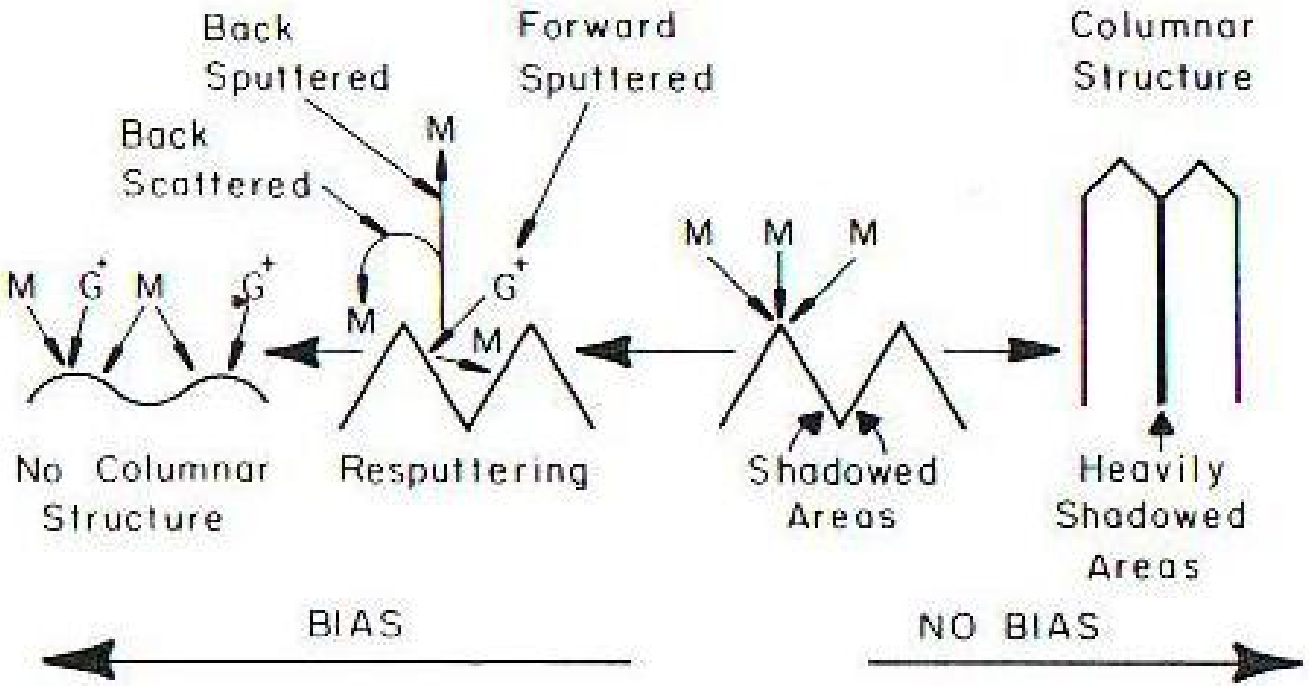

Fig. 6. Growth modification by ion bombardment during deposition. Reprinted with permission from American Institute of Physics, after R. D. Bland, G. J. Kominiak, and D. M. Mattox, *Journal of Vacuum Science & Technology* **VII**(4), 671–674 (1984).

Filtered cathodic arc deposition system

-We need to eliminate droplets in the films by magnetic filter

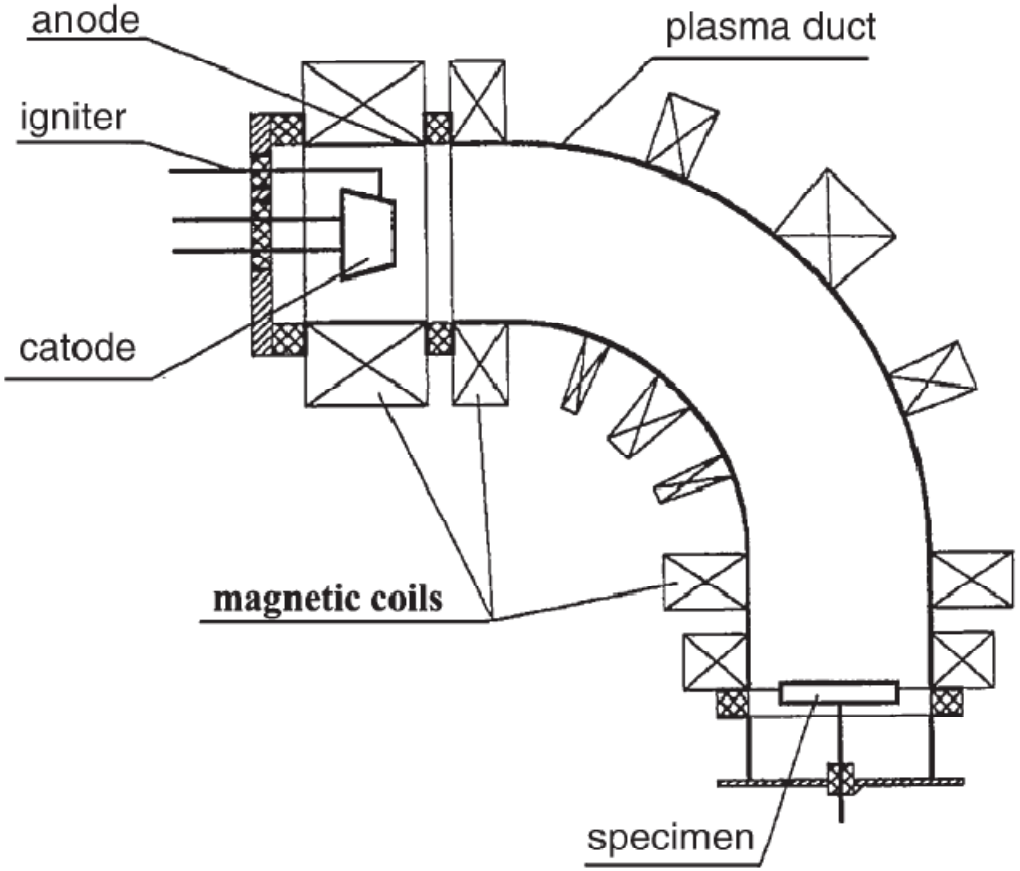

Fig. 25. A schematic diagram of a cathode arc source with a 90°-duct filter (from Karpov [145]).

-This is observed to develop extreme residual stress in coatings with values routinely reaching 15 Gpa in filtered arc deposition system. It can be reduced by substrate bias application and ion bombardment control.

Othon R Monteiro, Annu. Rev. Mater. Res. 2001. 31:111–37

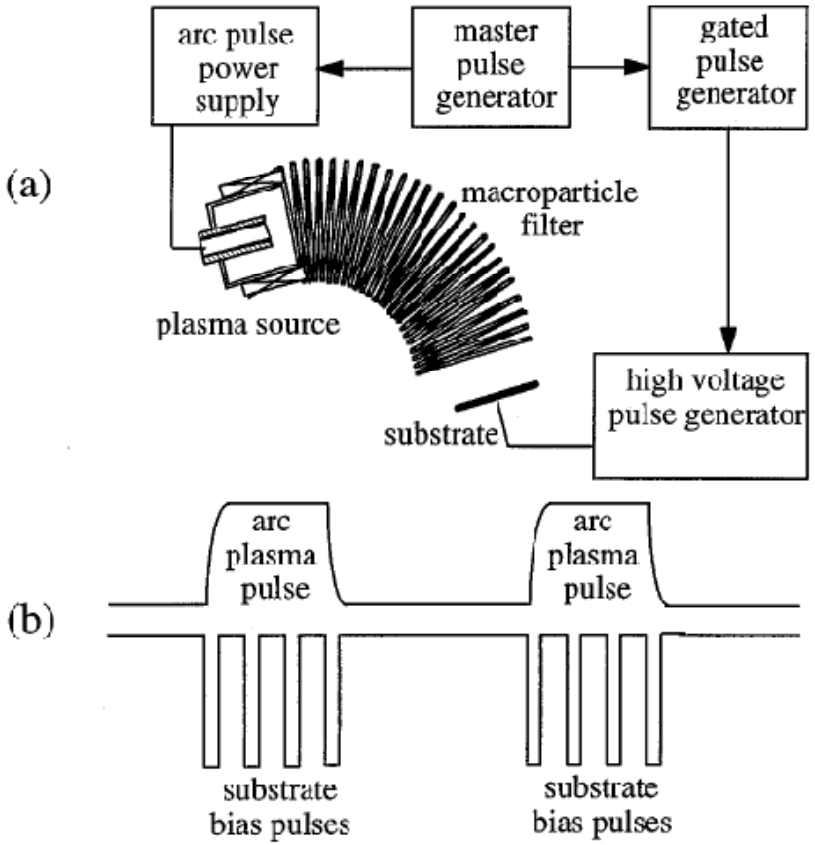

Figure 5 Schematic representation of metal plasma ion immersion implantation and deposition process.

F. Koch, Journal of Nuclear Materials 329–333 (2004) 1403–1406

Al_2O_3 and Er_2O_3 deposited by filtered arc for fusion applicati

-Evaporation of metallic cathodes is used and oxygen is added to arc plasma.

-RF induced DC bias on the substrate is used in order to control ion energy

-Deuterium permeation was measured for these coatings deposited on PdAg30 substrates

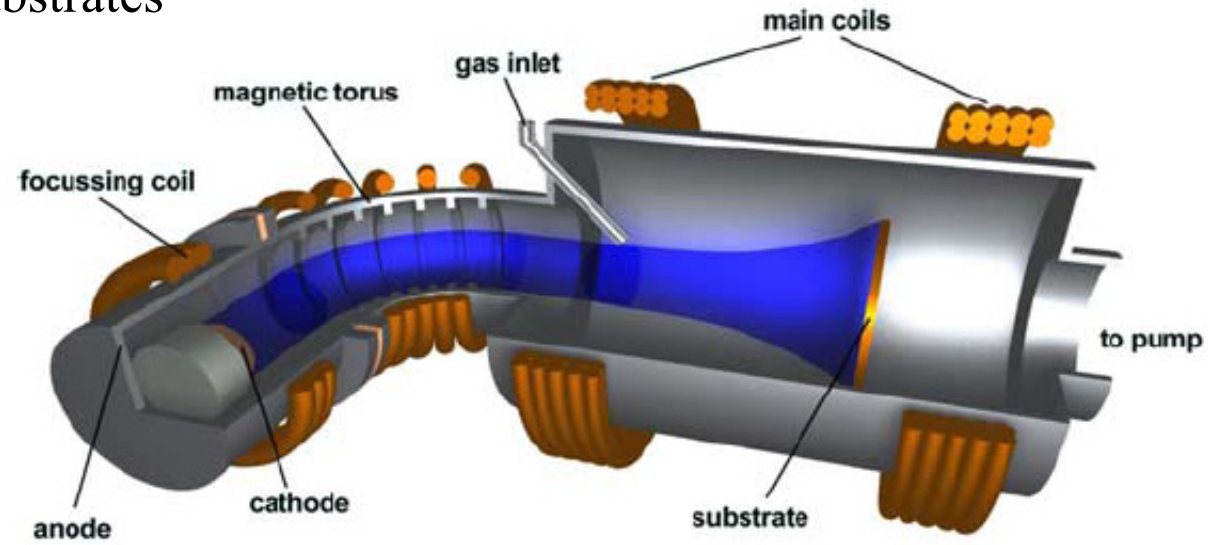

Fig. 1. Vacuum arc setup with toroidal filter system.

F. Koch, Journal of Nuclear Materials 329–333 (2004) 1403–1406

Results of ceramic coating deposition by filtered arc.

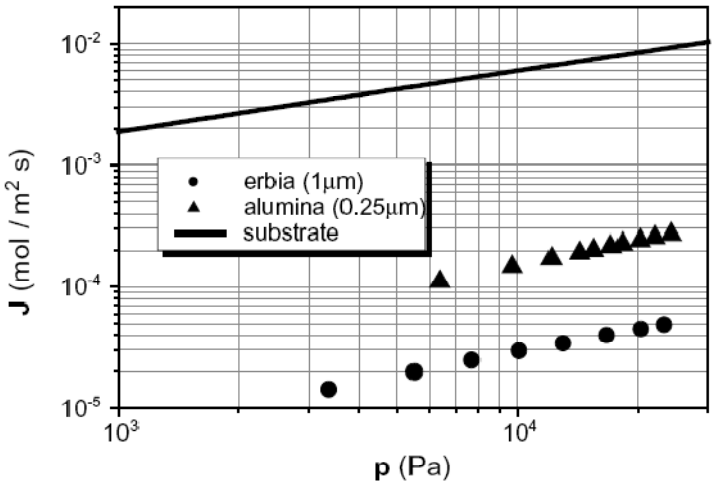

Fig. 5. Results from deuterium permeation experiments. The solid line corresponds to D permeation through an uncoated PdAg30 substrate. The triangles correspond to an Al_2O_3 coating deposited at 873 K without bias voltage. The circles correspond to Er_2O_3 deposited at 520 °C without bias voltage.

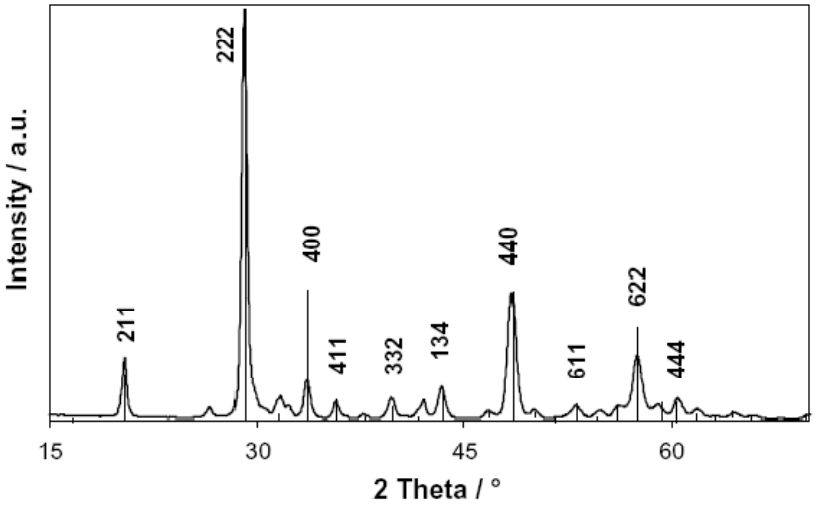

Fig. 3. XRD spectrum of an erbia film deposited at 570 °C with a bias voltage of −150 V. The vertical lines denote the amplitudes and angles of a calculated database powder diffraction file [15].